Journal of Photoscience (2003), Vol. 10(1), pp. 127−148

Weak Interactions Between Organic Molecules and Alkali Metal Ions Present in Zeolites Help Manipulate the Excited State Behavior of Organic Molecules

V. Ramamurthy*
Department of Chemistry, Tulane University, New Orleans, LA 70118

Zeolite is a porous highly interactive matrix. Zeolitic cations help to generate triplets from molecules that possess poor intersystem crossing efficiency. Certain zeolites act as electron acceptors and thus can spontaneously generate radical cations. Zeolites also act as proton donors and thus yield carbocations without any additional reagents. These reactive species, radical cations and carbocations, have long lifetime within a zeolite and thus lend themseleves to be handled as 'regular' chemicals. Internal structure of zeolites is studded with cations, the counter-ions of the anionic framework. The internal constrained structure and the cations serve as handles for chemists to control the behavior of guest molecules included within zeolites.

key words: Zeolites, Cation-π interaction, Chiral photochemistry, Singlet oxygen

INTRODUCTION

Being inspired by and having realized the complexity of natural systems, chemists have utilized a number of organized/confined media to study the photochemical and photophysical behavior of guest molecules [1-3]. Examples of organized media in which the guest molecules behavior has been investigated include molecular crystals, inclusion complexes (both in the solid and solution states), liquid crystals, micelles and related assemblies, monolayers, LB films, surfaces and natural systems such as DNA. In this article a partial overview of the activities in our laboratory, utilizing zeolite as a medium for photochemical and photophysical studies, is presented.

Structure and Properties of the Medium. Zeolites. Structure. Most of our studies have utilized faujasites and pentasils as the media. Zeolites in general may be regarded as open structures of silica in which aluminum has been substituted in a well-defined fraction of the tetrahedral sites [4-8]. The frameworks thus obtained contain pores, channels and cages of different dimensions and shapes. The substitution of trivalent aluminum ions for a fraction of the tetravalent silicon ions at lattice positions results in a network that bears a net negative charge which is compensated by positively charged counter ions. The topological structure of X- and Y-type zeolites (faujasites) consists of an interconnected three dimensional network of relatively large spherical cavities, termed supercages (diameter of about 13.4 Å; Figure 1). Each supercage is connected tetrahedrally to four other supercages through 7.6 Å windows or pores. Charge-compensating cations present in the internal structure of X and Y zeolites are known to occupy three different positions; the first type (site I), with 16 cations per unit cell (both X and Y), is located on the hexagonal prism faces between the sodalite units. The second type (site II), with 32 per unit cell (both X and Y), is located in the open hexagonal faces. The third type (site III), with 38 per unit cell in the case of X type and only eight per unit cell in the case of Y type, is located on the walls of the larger cavity. Only cations at sites II and III are expected to be readily accessible to the organic molecule adsorbed within a supercage. Charge compensating cations are exchangeable and such an exchange brings along with it a variation in a number of physical characteristics such as electrostatic potential and electric field within the cage, the spin-orbit coupling parameter and the vacant space available for the guest within the supercage.

Pentasil zeolites (ZSM-5 and ZSM-11) also have three-dimensional pore structures (Figure 1); a major difference between the pentasil pore structures and the faujasites described above is the fact that the pentasil pores do not link cage structures as such. Instead, the pentasils are composed of two intersecting channel systems. For ZSM-5, one system consists of straight channels with a free diameter of about 5.4×5.6 Å and the other consists of sinusoidal channels with a free diameter of about 5.1×5.5 Å. For ZSM-11, both are straight channels with dimensions of about 5.3×5.4 Å. The volume at the intersections of these channels is estimated to be 370 $Å^3$ for a free diameter of about 8.9 Å.

Zeolite as a Reaction Cavity. Characteristics. One is accustomed to carrying out reactions in large reaction vessels that are disproportionately larger than the size of a molecule. However, when the size of the reaction vessel is

---

*To whom correspondence should be addressed.
E-mail : murthy@tulane.edu
Received & Accepted; October 23, 2002

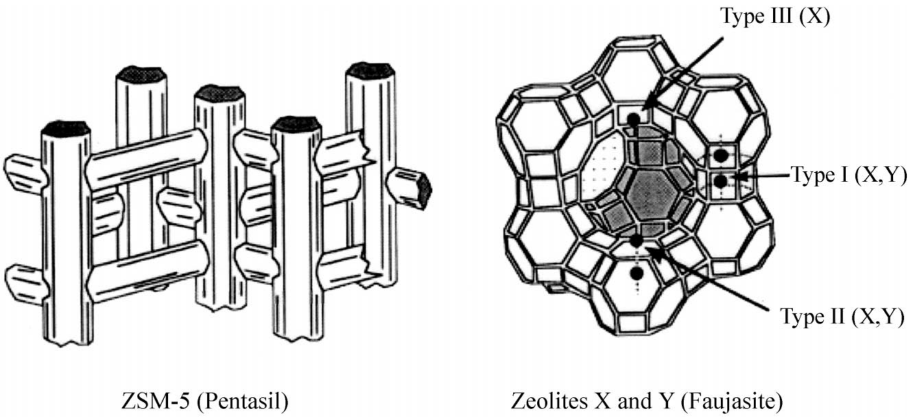

Figure 1. Structures of Zeolites: ZSM-5 and Faujasites (X and Y). Position of cations in X and Y zeolites shown as Type I, II and III.

nearly the same as that of the reactant molecule, one will have to consider factors that might normally be ignored. While a photochemical macromolecular reactor, such as a quartz cuvette, should play no role on the photochemical events occurring on the substrate of interest, a molecular-sized enclosure would be capable of influencing the reactivity of the substrate. Zeolites similar to glasses and quartz vessels are made up of silica and alumina and therefore, generally one should be able to excite an organic molecule without perturbing the electronic structure of the zeolite.

Reactions taking place within a zeolite can be envisioned to occur within an enclosed space which we call as a ‘reaction cavity’ [9,10]. The term ‘reaction cavity’ was originally used by Cohen to describe reactions in crystals [11]. He identified the reaction cavity as the space occupied by the reacting partners in crystals and used this model to provide a deeper understanding of the topochemical control of their reactions. Selectivity seen for reactions in crystals, according to this model, arises due to lattice restraints on the motions of the atoms in reactant molecules within the reaction cavity. In other words, severe distortion of the reaction cavity will not be tolerated and only reactions that proceed without much distortion of the cavity are allowed in a crystal (Figure 2). Crystals possess time independent structures; the atoms that form the walls of the reaction cavity are fairly rigid and exhibit only limited motions (*e.g.*, lattice vibrational modes) during the time periods necessary to convert excited state molecules to their photoproducts. Therefore, in the Cohen model, the space required to accommodate the displacement of reactant atoms from their original positions during a chemical reaction must be built largely into the reaction cavity. Packing of polyatomic molecules in crystals leaves some distances between neighboring non-bonded atoms greater than the sum of their Van der Waals radii. This creates a certain amount of *free volume*, which may be so disposed as to allow the atomic motions required to effect a reaction. In the usual case, a reaction product will also place some stress on the host crystal as is evidenced by the fact that crystals such as those studied by Schmidt and Cohen are usually reduced to powders as the reaction progresses.

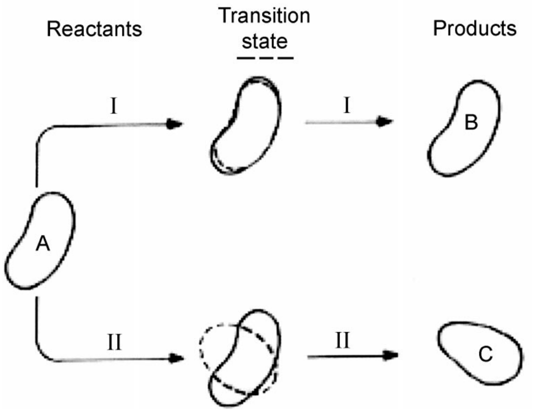

Figure 2. The reaction cavity of a favorable (I) and unfavorable reaction (II) in an organized medium. Large shape change in II is resisted by the medium.

Can we extend the above reaction cavity concept, which emphasizes the shape changes that occur as the reactant guest transforms itself to the product, to understand and predict the photobehavior of guest molecules included within a zeolite? We believe that such an extension should be possible with some limitations. The concept of reaction cavity will serve well as a vehicle for discussion of results obtained in media in which organized structures of hosts have significant effects on the photochemical response to excitation of guests. A reaction cavity is defined in terms of the factors such as ‘hard’ and ‘soft’ and ‘active’ and ‘passive’ and ‘free volume’. The concept of free volume is introduced into the reaction cavity model to accommodate the shape changes that occur as the reactants transform themselves to products. For example, the shape and the free volume of the supercage within X and Y zeolites will decide to some extent the nature of the product that is obtained from a guest molecule. The volume available for an organic molecule within a supercage depends on the number and nature

Table 1. Cation dependence of supercage free volume in MY zeolites

Cation (M^+)	Ionic Radius of the Cation (Å)[a]	Vacant Space[b] within the Supercage ($Å^3$)	
		Y-Zeolite	X-Zeolite
Li	0.6	834	873
Na	0.95	827	852
K	1.33	807	800
Rb	1.48	796	770
Cs	1.69	781	732

[a] R.J. Ward, *J. Catalysis*, **1968**, *10*, 34.

[b] Calculations of polyhedral volumes were performed using a modification of the POLYVOL Program [D. Swanson, R. C. Peterson, *The Canadian Mineralogist*, **1980**, *18*(2), 153; D. K. Swanson, R. C. Peterson, *POLYVOL Program Documentation*, Virginia Polytechnic Institute, Blacksburg, VA] assuming the radius of the TO_2 unit to be 2.08Å (equivalent to that of quartz).

of the cation. As the calculated supercage volumes given in Table 1 show, the available volume for a guest decreases as the cation size increases from Li^+ to Cs^+ [12]. Since surfaces of zeolites, possess time independent structures like crystalline materials, the free volume needed to accommodate shape changes which occur during the course of a reaction must be present intrinsically within the fixed structure. Reaction cavities of such media possess “hard” walls. Therefore it becomes very important to choose a proper zeolite (with adequate free volume) to steer a reaction towards a particular product.

The above model leads one to conclude that ‘guests in hosts’ are similar to balls in boxes. But this analogy is very deficient. In addition to being ‘hard’ or ‘soft’, cavity walls must be characterized as ‘active’ or ‘passive’. A zeolite reaction cavity has been characterized to be ‘active’. When the interaction between a guest molecule and the cavity is attractive or repulsive, the cavity is termed ‘active’ and when there is no significant interaction it is considered to be ‘passive’. Interactions may vary from weak van der Waal’s forces, to hydrogen bonds to strong electrostatic forces between charged centers. Zeolite surfaces contain a large number of cations which can interact electrostatically with guests. Thus the cation-guest interactions are expected to play a very significant role in controlling the fate of an excited molecule. Factors that determine the photochemical processes of a guest in a confined space include structural aspects of both the guest and the host zeolite and the nature of chemical and physical interactions between the two.

Zeolite as a Spectroscopic Matrix

Photochemistry of triplets of organic molecules is a well-developed field [13]. Despite its maturity, encountering systems whose photophysical behavior is not as expected is not uncommon. For example one might face a frustrating situation of being unable to observe phosphorescence from molecules of interest. Photochemists are also interested in characterizing the reactive intermediates that might arise in a photochemical reaction. True to their name these intermediates have a fleeting existence. In recent years zeolites have been shown to be very useful matrices for generating, stabilizing and observing reactive species such as triplets, radical cations, radicals and carbocations. Results from our laboratory are highlighted below to impress upon the readers the potential of zeolite as a matrix to observe species of interest to photochemists.

Triplets

Phosphorescence emission from organic molecules has been known since the last century [14]. Although very early reports of phosphorescence from dye molecules used a solid gel as the matrix, low temperature organic solvent glasses have been the primary choice for observation of phosphorescence from organic molecules [15]. While organic glasses are well accepted media, they pose limitations such as requiring the experiments be carried out at liquid nitrogen temperature and incorporation of only small amounts of heavy atom solvents before an organic glass becomes opaque. In the last two decades alternate matrices (silica gel, alumina, sucrose, chalk, paper, polymers, micelles, and cyclodextrins) have been explored to record phosphorescence [16,17]. In a number of these media phosphorescence even at room temperature has been observed. Occasionally heavy cation salts (eg., thallium, silver and lead salts) are incorporated to enhance the emission process. However, studies have been mostly restricted to aromatic compounds. We have established that zeolite is a powerful matrix to observe phosphorescence from organic molecules, even from those that do not phosphoresce under normal conditions [18-22]. The potential of this technique is illustrated with three examples, aromatics, polyenes and azo compounds. Of the three sets of molecules, olefins and azo compounds rarely phosphoresce.

As shown in Figure 3, the emission spectrum of naphthalene

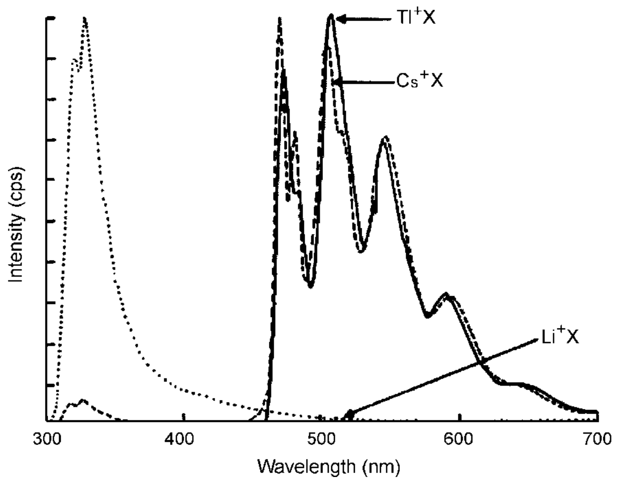

Figure 3. Emission spectra of naphthalene included within cation exchanged X zeolite at 77° K. Note the relative intensities of fluorescence and phosphorecence vary with the cation.

Table 2. Photophysical parameters for Naphthalene Included in Zeolites

Zeolite	Triplet Lifetime[a] (s)	Singlet Lifetime[b] (ns)	P/F[c]
Li X	–	33.0	1.0×10^{-4}
Na X	–	35.4	7.3×10^{-2}
K X	1.72	19.4	0.16
Rb X	0.72	2.22	8.1
Cs X	0.20	0.23(87%), 1.87(13%)	45
Tl X	0.0012	–	only P
Li Y	–	31.8	1.2×10^{-3}
Na Y	–	25.1	1.0×10^{-3}
K Y	–	13.8	0.1
Rb Y	–	3.8	9.0
Cs Y	–	0.7	60

[a] The lifetime measured at 77 K.

[b] The lifetime measured at 298 K.

[c] Phosphorescence to fluorescence intensity ratio estimated at 77 K; the number is independent of the wavelength of excitation.

Table 3. Estimated Spin-Orbit Coupling Constants for Metal cations and the isoelectronic Noble Gas Atoms[a,b]

Cation (isoelectronic noble gas)	Electronic configuration	Spin-orbit coupling constant ζ/cm^{-1}
Li^+ (He)	$1s^2$	0.7
Na^+ (Ne)	$1s^2\ 2s^2\ 2p^6$	520
K^+ (Ar)	$1s^2\ 2s^2\ 2p^6\ 3s^2\ 3p^6$	940
Rb^+ (Kr)	$1s^2\ 2s^2\ 2p^6\ 3s^2\ 3p^6\ 4s^2\ 4p^6$	3480
Cs^+ (Xe)	$1s^2\ 2s^2\ 2p^6\ 3s^2\ 3p^6\ 4s^2\ 4p^6\ 5s^2\ 5p^6$	6080
Li		0.23
Na		11.5
K		38
Rb		160
Cs		370

a. for cations the values are adopted from M. A. Anderson and C. B. Grissom, *J. Am. Chem. Soc.*, **1996**, *118*, 9552.

b. for neutral atoms the values are taken from S. L. Murov, I. Carmichael and G. L. Hug, Handbook of Photochemistry, Marcel Dekker: New York, 1993; p. 339.

is profoundly affected by inclusion in faujasites. For low-mass cations such as Li^+ and Na^+, the emission spectra show the typical naphthalene blue fluorescence. However, as the mass of the cation increases (e.g., from Rb^+ to Cs^+ to Tl^+), there is a dramatic decrease in fluorescence intensity and a simultaneous appearance of a new vibronically structured low-energy emission band that is readily identified as the phosphorescence of naphthalene. Table 2 lists excited singlet (at room temperature) and triplet lifetimes (at 77 K) of naphthalene included within various cation exchanged zeolites. It is clear that both these lifetimes are cation dependent. As tabulated in Table 3 the spin-orbit coupling parameter of the cation increases with the atomic weight. On the basis of the following observations we conclude that the heavy-cation effect is responsible for the enhanced phosphorescence and decreased singlet and triplet lifetimes for naphthalene within K, Rb, Cs and Tl cation exchanged faujasites. It is well-known that the effect of external heavy-atom perturbation scales with the square of the perturber's spin-orbit coupling constant, ξ^2 and that a log-log plot of τT^{-1} *vs.* ξ^2 should be linear with a maximum predicted slope of unity. As shown in Figure 4, the expected dependence is observed. For comparison, we have also provided in Figure 4 the linear relationship observed in two systems, namely 1-halonaphthalenes and 1,5-naphtho-22-crown-6, where the external and internal heavy-atom effects, respectively, are presumed to operate. The magnitude of the heavy-atom effect observed in zeolites is significantly larger than that observed for the 1,5-naphtho-22-crown-6 exchanged with heavy-atom cations where the cation is rigidly held over the naphthalene π-face. In fact the zeolite samples show heavy-atom effects nearly as large as for a series of 1-halonaphthalenes where the perturbers are covalently attached to the chromophore. This is attributable both to the close approach between naphthalene and the heavy atom which is enforced by the zeolite supercage and to the presence of more than one heavy-atom cation per supercage which leads to highly effective concentrations of the heavy-atom cation in the vicinity of the naphthalene molecule. If the heavy-cation effect is indeed responsible for the variations in singlet and triplet lifetimes, one would expect a linear relationship between singlet and triplet decays with cation variation. Indeed this is observed. Further support for the importance of heavy cation in enhancing the phosphorescence come from the dependence of the ratio of fluorescence to phosphorescence on the Cs^+ to Na^+ content in a zeolite. As seen Figure 5 the phosphorescence intensity increases with the Cs^+ ion content.

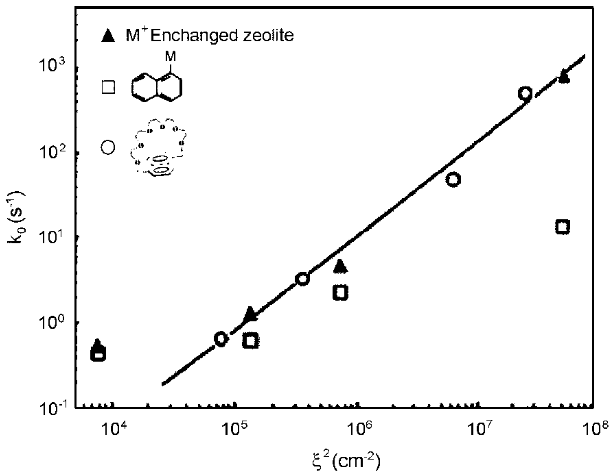

Figure 4. Dependence of excited state triplet lifetime on the spin-orbit coupling parameter of the cation. A comparison between crown ether systems, zeolites and 1-halonaphthalenes is provided.

The above effect is found to be general. Intense phosphorescence is observed for a wide range of different organic

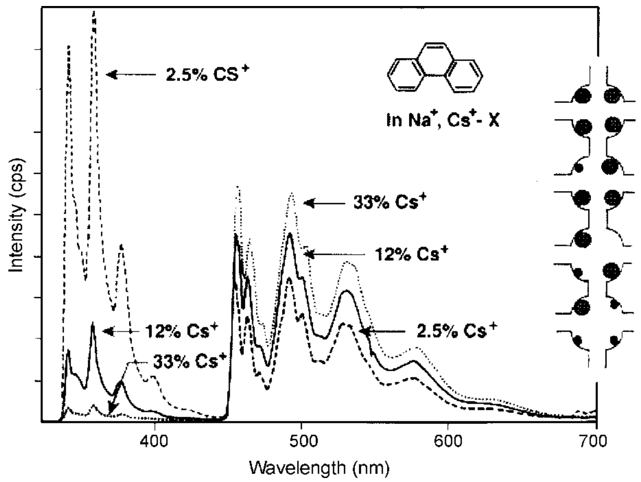

Figure 5. Emission spectra of phenanthrene included in Na, CsX. Note the dependence of the fluorescence to phosphorescence intensity on the % of Cs^+.

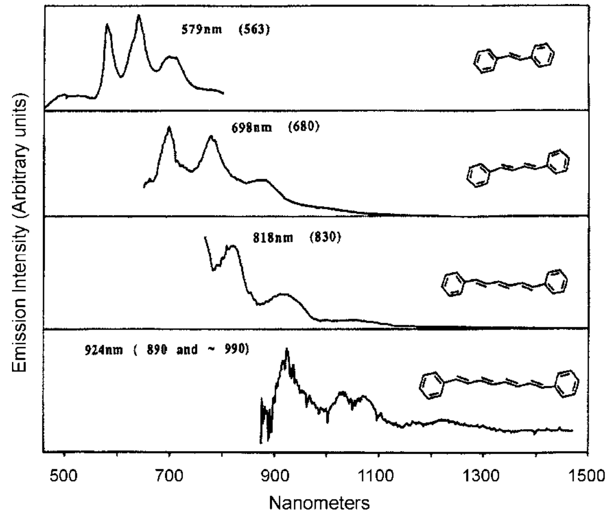

Figure 6. Phosphorescence spectra of all *trans*-diphenylpolyenes included within Tl^+ZSM-5 at 77°K.

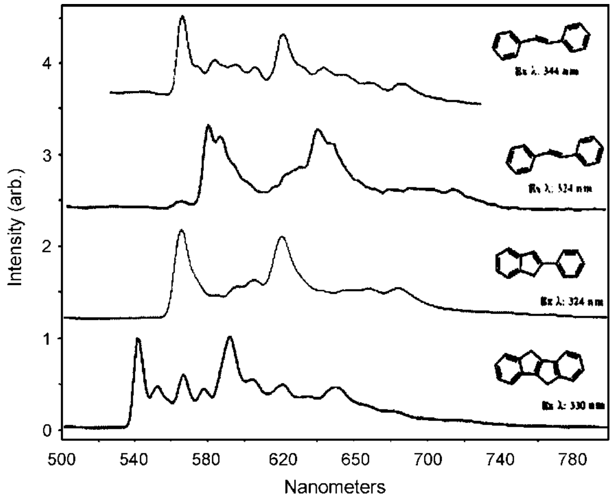

Figure 7. Phosphorescence spectra (at 77K) of *trans*-stilbene, phenylindene and indenoindene included in TlZSM-5. Note the variation in emission wavelength in the case of *trans*-stilbene with respect to excitation wavelength.

guests such as anthracene, acenaphthene, phenanthrene, chrysene, fluoranthene, pyrene, and 1,2,3,6,7,8-hexahydropyrene when included in Tl^+-exchanged faujasites. Fused aromatics, with too large a diameter to fit through the 8 Å windows of the X- and Y-type zeolites (e.g., coronene and triphenylene) do not show any phosphorescence when included within a zeolite.

The unique feature of this method is that one is able to observe phosphorescence from systems, which commonly fail to show this emission in organic glassy matrices even when they are subjected to heavy atom effect. Olefinic systems that under normal conditions do not show phosphorescence emit from their triplet states when included in Tl^+-exchanged zeolites. All-*trans*-α,ω-diphenylpolyenes exhibit very low intersystem crossing efficiencies and efficient fluorescence. We have succeeded in recording phosphorescence of these α,ω-diphenylpolyenes by including them in Tl^+-exchanged zeolites. Figure 6 shows the observed phosphorescence of the α,ω-diphenylpolyenes included in TlX. The singlet-triplet energy gaps (ΔT_1->S_0) obtained from the observed zero-zero lines are in excellent agreement with literature predictions. A point to note is that the wavelengths of phosphorescence from *trans*-stilbene is slightly dependent on the excitation wavelength (Figure 7). This we believe is due to the heterogenity of the sites present within a zeolite. Stilbene molecules, most likely, are present in various conformations within a zeolite and they do not interconvert in the time scale of the emission.

The remarkable ability of zeolites to turn on phosphorescence is related to the spin orbit coupling parameter of the cations Cs^+, Tl^+ and Pb^+. It should be noted that just grinding the cation salt with organic molecules does not result in phosphorescence. Zeolite structure favors intimate interaction between cations and the included organic molecules. One could view the zeolite structure as an expanded crystal lattice of a cation salt. While in a powdered cation salt only the cations at the surface interact with an organic molecule, within a zeolite almost every cation is able to interact with the organic molecule.

The above observations demonstrate the 'power' of a zeolite as a new and versatile medium for 'turning on' the external heavy-atom perturbation of organic molecules in which intersystem crossing (ISC) occurs between ππ* states. The rules for ISC, proposed by El Sayed suggest that heavy atom effect should be observable even in systems in which ISC occurs between the singlet and triplet states of nπ* character (Figure 8) [23]. Preliminary studies suggest that this is possible. The two systems we have examined in this context are alkanones and azo compounds both of which have been established to undergo ISC from nπ* singlet to pure nπ* triplet states (no

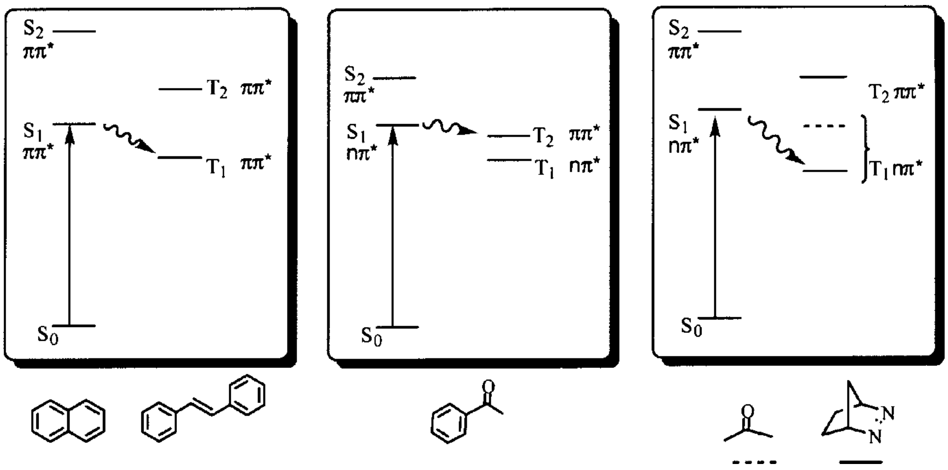

Figure 8. Possible scenarios for intersystem crossing between S_1 to T_1.

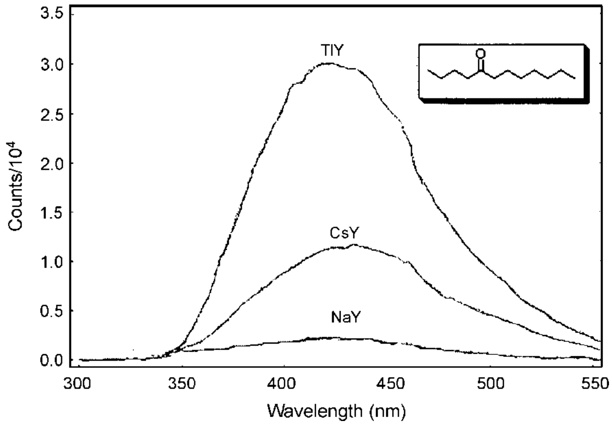

Figure 9. Phosphorescence spectra of 5-dodecanone included within NaY, CsY and TlY. Emission recorded at 77°K. Note the enhancement in phosphorescence intensity with the heavier cation.

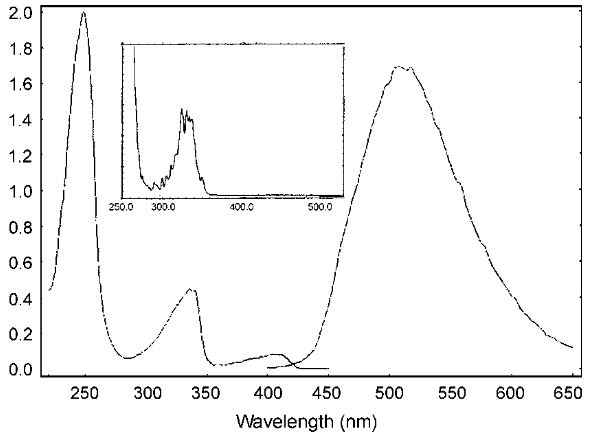

Figure 10. Emission and excitation spectra of diazo-(2,3)-bicycloheptane included within TlY, recorded at 77°K. Insert shows the diffuse reflectance absorption spectrum. The emission on the right is assigned to be phosphorescence. The longest wavelength band in the excitation spectrum is believed to be S_0 to T_1 transition.

other states lie between them).

Alkanones show both fluorescence and phosphorescence. In spite of the nπ* character of both S_1 and T_1 the small energy gap is believed to favor ISC between these states. Examination of the emission characteristics of a few alkanones showed that the ratio of phosphorescence to fluorescence is higher in TlY than in NaY (Figure 9). This observation indicated that a zeolite could influence the ISC between an nπ* singlet and an nπ* triplet. Results obtained with the azo compounds support the above conclusion. Numerous studies on azo compounds have established that they possess very poor ISC and do not show phosphorescence at 77K even in the presence of a heavy atom perturber. The lack of ISC has been attributed to the presence of a large energy gap (>15 kcal/mole) and to the nπ* character of the excited states involved in ISC. A number of azo compounds that are reported to show no phosphorescence in organic glass surprisingly showed phosphorescence within a TlY zeolite [24]. One such example is provided in Figure 10.

Radical Cations

Radical cations play an important role in photoinduced electron transfer chemistry. Although spectral characterization of radical ions by time resolved laser spectroscopy is possible characterization by ESR requires sufficiently long-lived radical ions. This is generally achieved by generating the radical ions within a solvent matrix (inert freon matrix) at low temperatures. Even in this matrix they have a relatively short lifetime (seconds). Silica gel, silica-alumina, and vycor glass have been explored as possible media to stabilize radical cations. During the last decade zeolites have emerged as a possible alternative to freon matrix to stabilize radical cations [25]. In this matrix radical cations have extended lifetimes (from hours to months). We serendipitously came across a phenomenon in which the

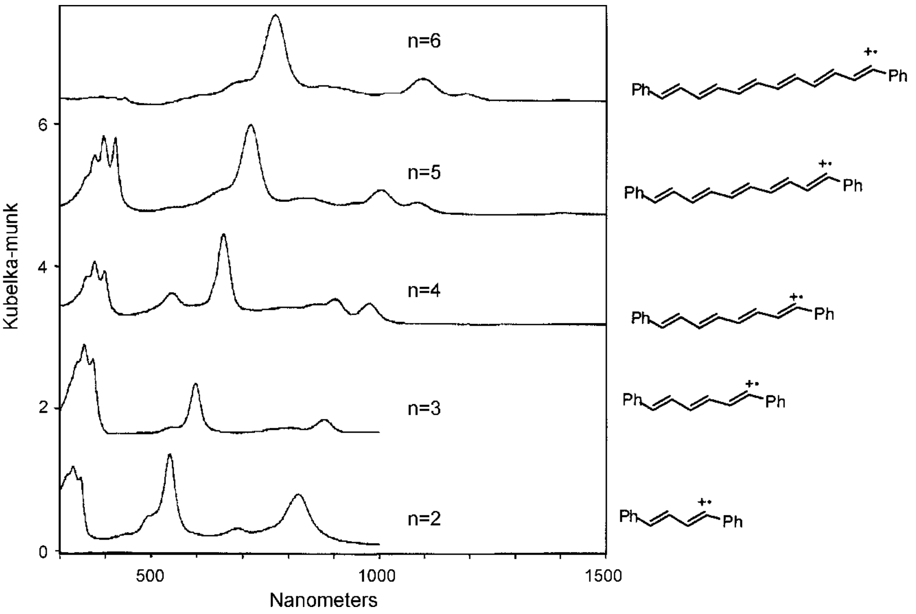

Figure 11. Diffuse reflectance spectra of diphenylpolyenes included within Na-ZSM-5. All spectra seen here correspond to the radical cations of the olefins.

radical ions generated spontaneously within a ZSM zeolite have lifetimes of the order of months [26-29].

When activated Na-ZSM-5 (Si/Al=22) was stirred with α,ω-diphenylpolyenes (trans-stilbene, diphenylbutadiene, diphenylhexatriene, diphenyloctatetraene, diphenyldecapentene, and diphenyldodecahexaene) in 2,2,4-trimethylpentane, the initially white zeolite and colorless to pale yellow olefins were transformed into highly colored solid complexes within few minutes. All the samples exhibited intense ESR signals with g values of 2.0028. Diffuse reflectance spectra of these powders (Figure 11) are identical to the spectra of the radical cations of α,ω-diphenylpolyenes reported in the literature. Diffuse reflectance and ESR results favor the conclusion that the colored species formed upon inclusion of α,ω-diphenylpolyenes in Na-ZSM-5 are radical cations. The colored α,ω-diphenylpolyene radical cations generated in the channels of Na-ZSM-5 were found to be unusually stable; even after several weeks of storage at ambient temperature in air, the colors persisted and the peak positions of the diffuse reflectance spectra remained unchanged. This is to be contrasted with their short lifetimes in solution (microseconds) and in solid matrices (seconds). The remarkable stability of these radical cations in Na-ZSM-5 derives from the tight fit of the rod-shaped molecules in the narrow zeolite channels; the π-orbitals are protected from external reagents by the phenyl rings which fit tightly in the channels at both ends of the radical.

We have been able to generate radical cations of thiophenes as well. When activated Na-ZSM-5 (Si/Al 22) was loaded with terthiophene a deep red-purple complex was obtained. Comparison of the diffuse reflectance spectrum of the above deep red purple complex with flash photolysis results where the terthiophene cation radical is generated as a transient in solution shows excellent agreement. As expected for a simple cation radical, an EPR spectrum for the above complex was observed although no hyperfine structure was resolved. The results obtained for terthiophene included in Na-ZSM-5 are not unique. The same type of one electron oxidation reaction for bithiophene and quaterthiophene included in ZSM-5 was observed (Figure 12). The stability of the cation radicals, which

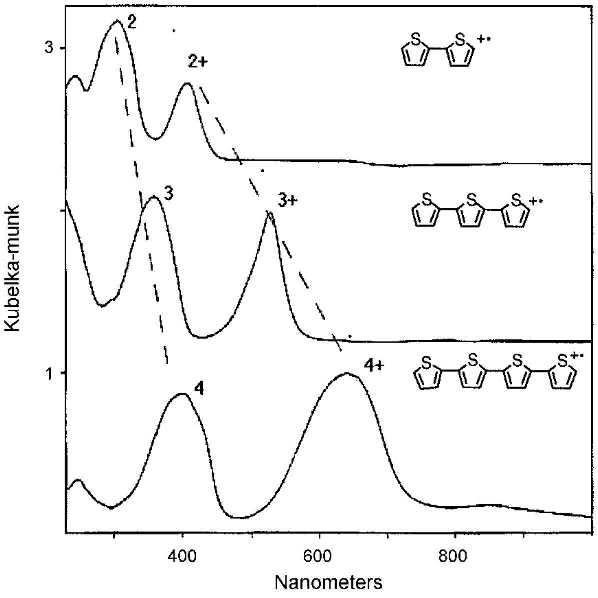

Figure 12. Radical cation formation of thiophene oligomers upon inclusion within Na-ZSM-5. Diffuse reflectance spectra of radical cations recorded at room temperature.

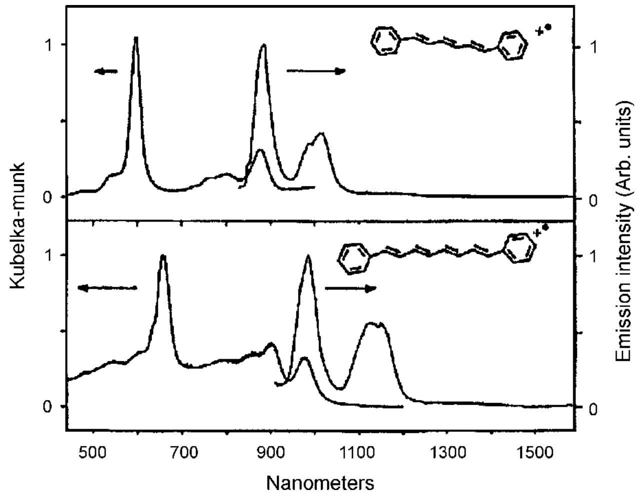

Figure 13. The emission spectra of the radical cations 1,6-diphenylhexatriene and 1,8-diphenyloctatetraene.

exist only as reactive intermediates in solution, is much higher within the zeolite channels; we have stored samples of the terthiophene cation radicals for months without any significant degradation even in the presence of air and water. Generation of radical cations of thiaanthrene, biphenyl, *para*-propylanisole, dithianes, and disulfides has been reported in the literature.

The ability to generate and stabilize radical cations of polyenes has helped us to handle them as routine chemicals rather than as intermediates. For example we have recorded the emission spectra of radical cations of α,ω-diphenylpolyenes as one would record that of parent α,ω-diphenylpolyenes (Figure 13).

Carbocations

One can generate and stabilize select carbocations within a zeolite [30-37]. Although this method is less general than the ones described above for triplets and radical cations, it can be useful in certain cases. A few examples are highlighted below. The best choice of zeolite for generation of carbocations is CaY. When activated CaY was added to a solution of 4-vinylanisole in hexane, the zeolite developed a vibrant red-violet color. The diffuse reflectance spectrum of the solid zeolite sample presented in Figure 14 consists of two broad absorptions centered at 340 and 580 nm. We attribute the absorption at ~340 nm to the carbocation, 4-methoxy phenylethyl cation. The absorption spectrum for 4-methoxy phenylethyl cation has been reported in solution and coincides remarkably well with the absorption maximum observed in zeolite. While 4-methoxy phenylethyl cation in solution lasts only for a few microseconds, in a zeolite it is stable for a few days.

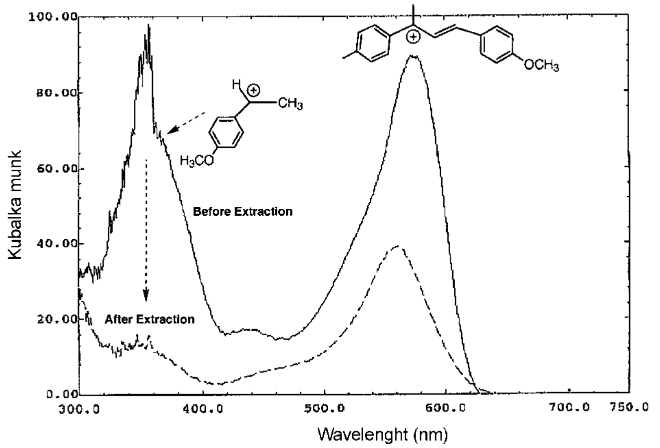

Figure 14. The diffuse reflectance spectra of the monomer and dimer cations of vinyl anisole included within CaY. The structures of the cations are shown. The monomer cation can be selectively washed away leaving the dimer cation within the zeolite.

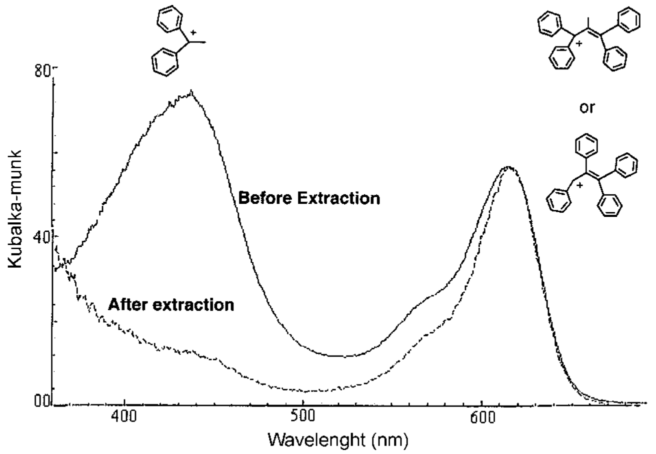

Figure 15. The diffuse reflectance spectra of the monomer and dimer cations of 1,1-diphenylethylene included within $Ca^{2+}Y$. The structures of the cations are shown. The monomer cation can be selectively washed away leaving the dimer cation within the zeolite. The exact structure of the dimer cations remains unresolved.

Behavior of diphenylethylene is similar to that of vinyl anisole. When activated CaY was added to a hexane solution of 1,1-diphenylethylene, the zeolite-hexane slurry turned yellow and then green and remained green for several days. The diffuse reflectance spectra displayed in Figure 15 for 1,1-diphenyl ethylene-Ca Y consist of two distinct maxima (one below 500 nm and the other above 600 nm). The absorption at 428 nm is attributed to diphenylmethyl cation. This is consistent with the literature assignment for such a species. Once again the cation has a few microseconds lifetime in solution while within a zeolite it is stable for days. The cation generation is spontaneous. Simple stirring in hexane or grinding zeolite with the olefin results in stable carbocation which require no special precaution for stabilization.

The monomer cations of vinyl anisole and diphenylethylene were found to slowly dimerize to small amounts of dimeric cations which lasts for months. The structures of the dimeric

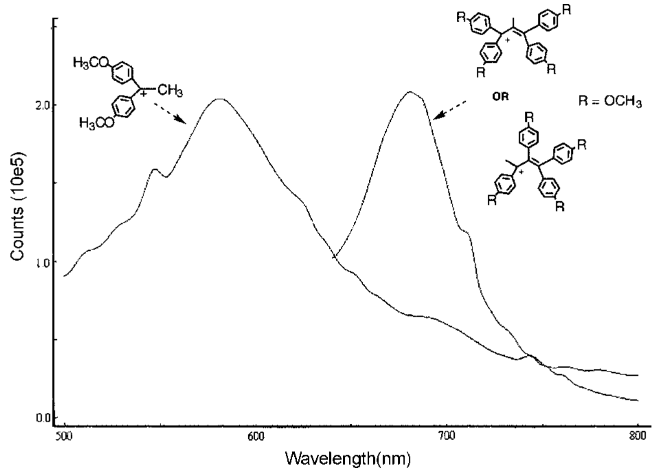

Figure 16. Fluorescence emission spectra of monomer and dimer carbocations of 1,1-dianisylethyelne included within $Ca^{2+}Y$ recorded at room temperature. The structures of carbocations are shown. The exact structure of the dimer cations remains unresolved.

cations are shown in Figures 14 and 15. The structure of the dimer cation from 1,1-diphenylethylene has not been conclusively established. What is important to note is that one can generate long-lived carbocations within a zeolite. The unusual ability to stabilize certain carbocations within zeolites has allowed us to handle them as 'normal' laboratory chemicals. For example we have been able to record emission from several of these cations. One such example is provided in Figure 16.

Zeolite as a Reaction Medium. Role of Cations

In this section we discuss how a 'small' (light) cation influences the photoprocesses of an organic guest molecule included within a zeolite. Small cations generate high electric field, polarize the electron distribution of a molecule by electrostatically interacting with the non-bonding and/or π-electrons of guest molecules and provide a high micropolarity.

State Switching in Carbonyl Compounds: Role of Cation-Carbonyl Interaction

We have noticed that one can control the reactivity of steroidal enones within zeolites [38-40]. We believe that the observed effects could be the result of the field generated by cations present within zeolites. Results on one steroid are presented below. In isotropic solution, androstenedione has been established to react mainly from the cyclopentanone D-ring. As illustrated in Scheme 1, the epimerization to yield 13-α-androstenedione is the major reaction in most solvents; only in 2-propanol reduction of the cyclohexenone A ring is able to compete with the epimerization process. Irradiation of androstenedione included in NaY gave only reduction product (Scheme 1); careful analysis at the initial stages of irradiation did not show the presence of the epimer. While this molecule reacts only from the cyclopentanone D ring in hexane, no products due to reactions from the D-ring are seen when it is included within NaY. This, we believe, is a reflection of the lowering of the energetics of the enone chromophore well below that of the cyclopentanone D ring. We suggest that

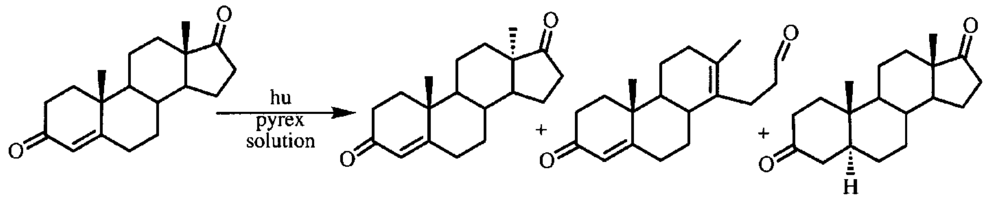

Hexane	40	4	–
Methylene Chloride	45	5	–
Methanol	42	4	–
Cyclohexane	36	3	–
2-Propanol	18	2	14
MCM-41 (Si/Al: >1000; Pure silica)	50 %		-
High Silica Y (Si/Al: >285)	30 %		-
Na X (Si/Al: 1. 2)	-		>90%
Na Y (Si/Al: 2. 5)	-		>85%

Scheme 1.

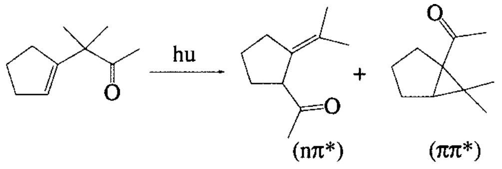

3 **4** **5**

hexane	100%	0%
methanol	78	22
acetonitrile	76	24
KX/hexane	25	75
KY/hexane	26	74

Scheme 2.

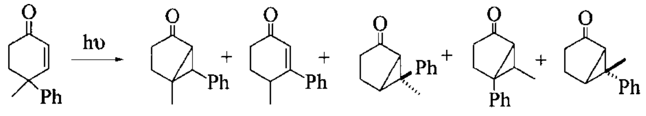

6 **7** **8** **9** **10** **11**

benzene	100%	0 %
ethanol	67	33
acetonitrile	58	42
LiY/hexane	13	87
NaY/hexane	30	70
NaX/hexane	29	71

Scheme 3.

lowering of the ππ* excited state of the A ring is responsible for the changes in reactivity of androstenedione included within NaY. Observed β-selectivity during the reduction of the enone C=C bond can also be rationalized on the basis of changes in the characteristics of lowest excited state. Chan and Schuster have established in the case of 4α-methyl-4,4α,9,10-terahydro-2(3H)phenanthrone, a molecule closely analogous to the systems investigated here, that reduction occurs stereospecifically from ππ* excited triplet to yield a cis fused bicyclic ketone. This would correspond to β-addition in our examples. Based on this analogy, one would suggest that the changes in the characteristics of the lowest excited triplet state of the enone chromophore discussed above is responsible for the observed selectivity.

Triplet sensitization of 3-methyl-3-(1-cyclopentenyl)butan-2-one, **3**, yields the 1,3-acyl migration product **4** from the nπ* triplet (and nπ* singlet) and the oxa-di-π-methane product **5** from the ππ* triplet (Scheme 2). Triplet sensitization of **3** by 4'-methoxyacetophenone in hexane gave exclusively the product from the nπ* triplet, **4**. However, in polar solvents, such as methanol and acetonitrile, a mixture of **4** and **5** was obtained (Scheme 2). The oxa-di-π-methane product 3 was obtained in higher yield within zeolite than in non-polar hexane or in other polar solvents used in this investigation. The selectivity in favor of the ππ* triplet product observed in zeolites is unmatched in any organic solvent, attesting to the uniqueness of zeolites.

The above strategy of controlling product distributions by inclusion in a zeolite also worked with 4-methyl-4-phenyl-2-cyclohexenone **6**. As shown in Scheme 3, of the several products (**7-11**) that this molecule gives upon excitation, **7** and **8** have been established to arise from the nπ* triplet and products **9-11** from the ππ* triplet. The ratio of the two sets of products [(**9**+**10**+**11**)/(**7**+**8**)] has been reported to depend on solvent polarity (Scheme 3). Similar to enone **3**, in non-polar hydrocarbon solvent, products from the nπ* triplet alone were obtained suggesting that the lowest triplet is of nπ* in character and the second ππ* triplet is not close enough to establish an equilibrium and react. With increasing polarity, the two states apparently are brought closer in energy such that products from both states are formed (Scheme 3). Consistent with the behavior of enone **3**, direct irradiation of **6** included within MY and MX zeolites gave higher yields of products **9-11** derived from the ππ* triplet (Scheme 3) than in non-polar benzene (0%) or moderately polar acetonitrile (42%). In LiY the combined yield of [(**9**+**10**+**11**)] was >85%, even higher than in 30% water-methanol mixture (75%). The results obtained in Y-Sil and MCM-41 (25% of [(**9**+**10**+**11**)]), zeolites with no cations, reveal the key role of cations in enhancing the yield of ππ* triplet products.

We believe that the cations present in zeolites play a direct role in the above state switching. This conclusion is supported by computational studies carried out with enones. The binding energies for Li$^+$ to formaldehyde and acetone have been experimentally measured to be ~36 and 45 kcal.mol^{-1}, respectively. Although the corresponding data for enones are not available, the values are likely to be in the same range. At the MP2/6-31G* level, we computed the binding energies of Li$^+$ to cyclopentenone and cyclohexenone to be 54 and 54.5 kcal.mol^{-1}, respectively (for reference, the corresponding value for acetone is computed to be 48 kcal.mol^{-1}). Although the strength of interaction is likely to be reduced due to the presence of oxyanionic counterions, enones adsorbed within a zeolite are expected to be bound to M$^+$ ions. We therefore probed the effect of metal complexation on the orbital and excitation energies of the model systems, cyclopentenone and cyclohexenone, along with acetone for comparison.

As in earlier studies on simple carbonyl compounds, the Li$^+$ ion is computed to be aligned nearly collinear with the C=O bond, suggesting a primarily ion-dipolar electrostatic interaction between the metal ion and the enone (Figure 17). While the nature and relative coefficients of the MOs are not altered in any significant manner, all the MOs are shifted to lower energies through coordination. The key MOs of importance in the present context are the p-type n orbital on the carbonyl oxygen, the filled π (higher lying π_2 for the enones) and the vacant π*

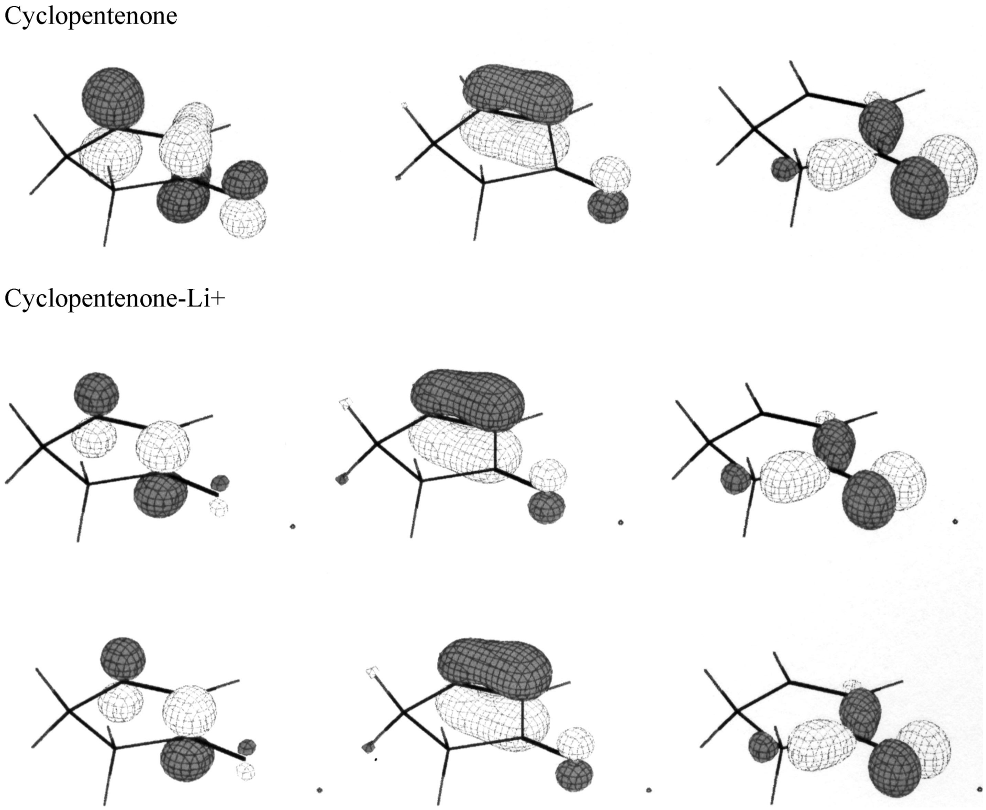

Figure 17. Schematic representations of (from right to left) n, π_2 and π^* orbitals of cyclopentenone (top) and cyclopentenone-Li$^+$ complex.

Table 4. Ground state orbital energies (HF/6-31G*) and energies of triplet states relative to the ground state (CIS(D)/6-31+G*) for carbonyl compounds and their Li$^+$ complexes

Molecule/Ion	Orbital Energy (eV)			Triplet Energy (eV)[a]	
	π	n	π^*	n-π^*	π-π^*
Acetone	-13.03	-11.19	4.28	4.04(4.41)	6.28(5.19)
Acetone+Li$^+$	-18.45	-16.67	-2.08	4.51(5.16)	6.63(6.38)
Cyclopentenone	-10.21	-10.86	2.93	3.69(4.33)	4.23(3.36)
Cyclopentenone+Li$^+$	-14.31	-15.99	-1.99	4.35(5.29)	4.10(3.43)
Cyclohexenone	-10.08	-10.90	2.80	3.50(4.13)	4.05(3.17
Cyclohexenone+Li$^+$	-14.03	-15.74	-2.02	4.15(5.11)	3.84(3.19)

[a] Results obtained at CIS/6-31+G* level (without doubles corrections) are given in parentheses

orbitals (shown in Figure 17 for cyclopentenone). The n orbital is stabilized by Li$^+$ complexation to a greater extent than the π MO in the model enones (Table 4), suggesting that the $n\pi^*$ triplet will be relatively shifted to higher energy due to cation binding. The CIS(D)/6-31+G* calculations confirm that the $n\pi^*$ triplet is the lowest energy triplet in the three model systems (Table 4). While this is expected for acetone on the basis of orbital energies, the trend prevails in the enones in spite of the fact that the n orbital is below the π_2 HOMO. More significant in the present context is the effect of Li$^+$ coordination on the energies of the triplet states. While the $n\pi^*$ triplet is clearly shifted to higher energy, the $\pi\pi^*$ triplet is marginally stabilized in the enones. The lower energy triplet is now calculated to be the $\pi\pi^*$ state. The switch in the ordering of the triplet states and their relative energies are both qualitatively consistent with the observed product selectivities in photoreactions of enones in zeolites. The fact that different ordering of $n\pi^*$ and $\pi\pi^*$ states are obtained at CIS and CIS(D) level suggests that cation free cyclopentenone the two states are very close. The nature of the lowest triplet of enones is very much dependent on the structure of the enone. For all the examples shown in Schemes 1-3 the lowest triplet in non-polar solvent is established to be $n\pi^*$ in character.

Consistent with the above speculations the emission spectra of acetophenones within NaY correspond to that of a $\pi\pi^*$ triplet state [41]. Acetophenone both in the singlet and triplet manifolds possesses close lying $n\pi^*$ and $\pi\pi^*$ excited states. Both in polar and non-polar solvents $n\pi^*$ triplet is the lowest excited state (Figure 18). We illustrate here that the influence of cations on the ordering of excited state can be easily inferred from the emission spectrum of the adsorbed ketone. Acetophenone, *para*-fluoroacetophenone, and *para*-methoxyacetophenone are chosen as examples. Based on the knowledge that a highly polar medium would be expected to increase the energy of the $n\pi^*$ state and lower the energy of the $\pi\pi^*$ state, one would predict that the lowest excited state of acetophenone and *para*-fluoroacetophenone could be altered

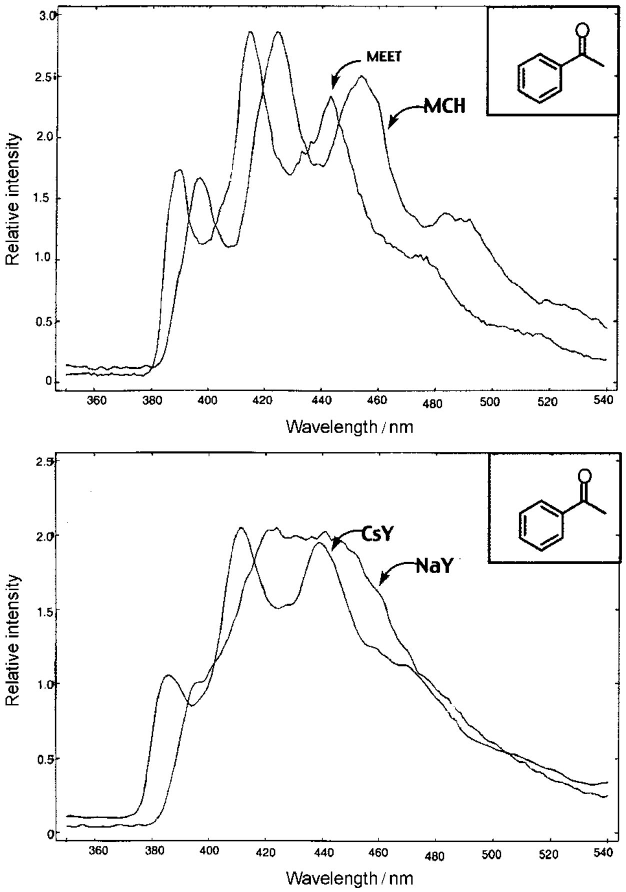

Figure 18. The emission spectra of acetophenone: (top) in methylcyclohexane (MCH) and methanol-ethanol mixture (MEET) at 77 K. (bottom) in NaY and CsY.

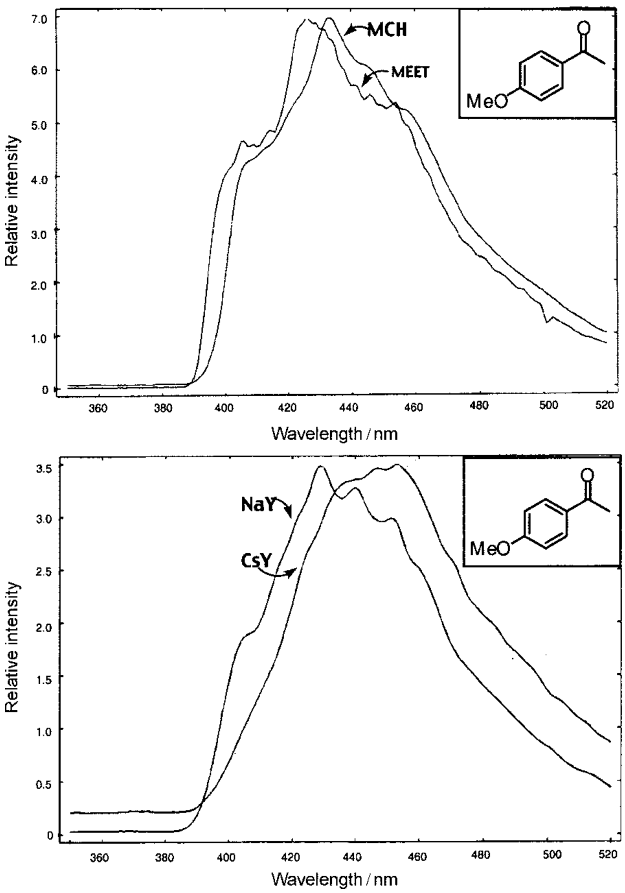

Figure 19. The emission spectra of *para*-methoxyacetophenone: (top) in methyl-cyclohexane (MCH) and methanol-ethanol mixture (MEET) at 77K. (bottom) in NaY and CsY.

within a zeolite while that of *para*-methoxyacetophenone will remain to be ππ* state in all solvents and in zeolites. Indeed the phosphorescence emission of *para*-methoxy acetophenone in NaY and CsY was structureless, characteristic of the ππ* state (Figure 19). On the other hand, the structural resolution of the phosphorescence emission from acetophenone was dependent on the cation. In NaY the emission was structureless, typical of ππ* emission and in CsY it was structured similar to that in methanol-ethanol mixture (Figure 18). Observations made with *para*-fluoroacetophenone were similar. Based on the appearance of the phosphorescence spectra we believe that both acetophenone and *para*-fluoroacetophenone possess ππ* excited states within NaY and nπ* state within CsY. Considering that these two ketones have nπ* state as their lowest excited triplet in the most polar solvent mixture, methanol-ethanol, the ability to switch the states within a zeolite using cations is novel and important.

Selectivity During Singlet Oxygen Mediated Oxidation of Olefins. Role of Cation-Olefin π Interaction

Singlet oxygen is known to react with electron-rich olefins via a 2+2 addition process. When the olefin contains allylic hydrogen atoms, however, the 'ene reaction' is the dominant pathway. Olefins with more than one distinct allylic hydrogen yield several hydroperoxides (Scheme 4). With a zeolite medium high selectivity during the singlet oxygen ene reaction has been achieved.

Monomeric thionin is a useful sensitizer for the generation of singlet oxygen. Singlet oxygen, generated using thionin included in a zeolite, is capable of undergoing an ene reaction with typical olefins such as 2,3-dimethyl-2-butene and 2-methyl-4,4-dimethyl-2-pentene. The product distribution observed with 1,2-dimethylcyclohexene suggests that the hydroperoxides so obtained are not the result of reaction with ground-state triplet oxygen (Scheme 5). These observations confirm that one can generate a reactive singlet oxygen within the confines of a zeolite [42-44]. A number of olefins of structure similar to 1-methyl-2-pentene were examined. These olefins contain two distinct allylic hydrogen atoms and, in an isotropic solution, yield two hydroperoxides with no appreciable selectivity (Scheme 6). Within NaY, a single hydroperoxide is preferentially obtained. Similar selectivity was also observed with related

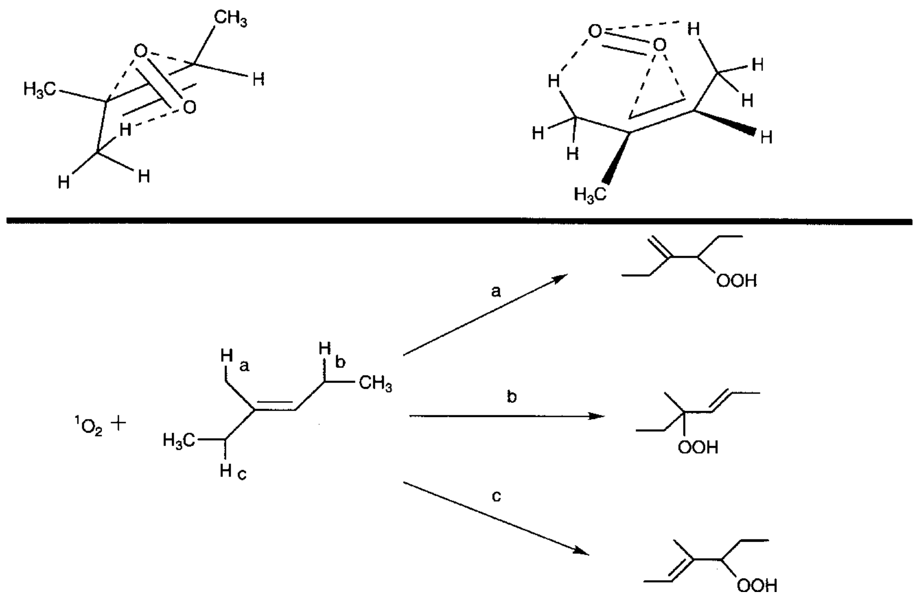

Scheme 4.

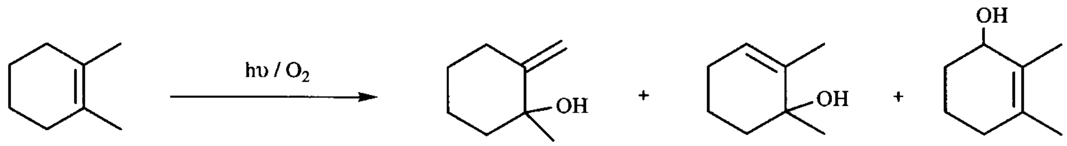

Conditions	Relative Yields		
Rose Bengal / Acetonitrile	89	11	0
Thionin/ Na Y/Hexane	90	10	0
Autooxidation	6	39	54

Scheme 5.

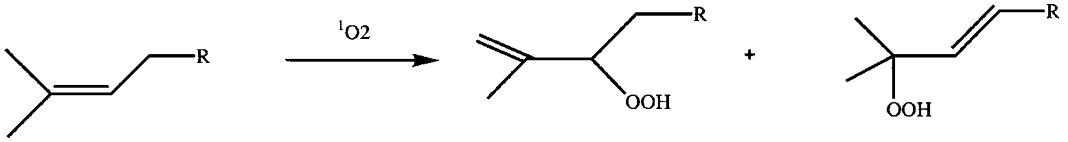

R = CH_3

Thionin/ CH_3CN	40	60
NaY/Thionin	100	--

R = $CH_2CH_2CH_3$

R = $CH_2(CH_2)_3CH_3$

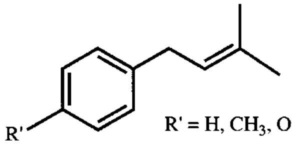

R' = H, CH_3, OCH_3

Scheme 6.

olefins such as the 1-methyl-4-aryl-2-butenes and even more impressive results were obtained with 1-methylcycloalkenes (Scheme 7). These alkenes yield three hydroperoxides in solution with the hydroperoxide resulting from abstraction of the methyl hydrogens formed in the lowest yield. Surprisingly, the minor isomer in solution was obtained in larger amounts

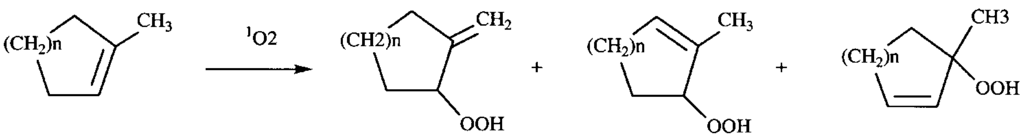

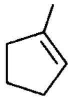	Thionin/CH$_3$CN	6	45	48
	Thionin/NaY/Hexane	100	--	--
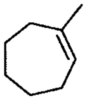	Thionin/CH$_3$CN	10	47	43
	Thionin/NaY/Hexane	100	--	--

Scheme 7.

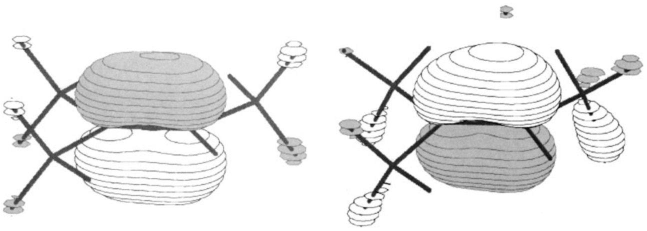

Figure 20. The π HOMO of 2-methyl-2-butene (left) and its Li$^+$ complex (right) calculated at the HF/6-31G** level.

within the zeolite. Thus the selectivity is a characteristic of hydroperoxidation of olefins within zeolites. Product hydroperoxides were isolated in ~75% yield.

The above selectivity is attributed to the polarization of the olefin by the interacting cation. As shown in Figure 20, when the olefin is asymmetric, the interacting cation will be able to polarize the olefin in such a way that the carbon with greater numbers of alkyl substituent will bear a partial positive charge (δ+). Singlet oxygen being electrophilic is expected to attack the electron rich carbon (δ–), the one with less substituents, and lead to an ene reaction in which the hydrogen abstraction will occur selectively from the alkyl group connected to the carbon bearing δ+. Polarization within a zeolite of molecules such as pyrene, NO, olefin-oxygen have been previously reported. In our system, the extent of polarizability will depend on the charge density of the cation. Smaller cations such as Li$^+$ would be expected to polarize the olefin more than larger cation such as Cs$^+$. As per this model, selectivity is expected to decrease from Li$^+$ to Cs$^+$. Consistent with both the above two models, observed selectivity decreases with the size of the cation (Scheme 8; Li$^+$>Na$^+$>K$^+$>Rb$^+$>Cs$^+$).

The above models assume that there is an interaction between the cation and the olefin and that the interaction energy decreases with the size of the cation. Ab-initio quantum mechanical calculations performed with several olefins clearly show a decreasing trend in the binding energy between the cation and the olefin, the smaller cations binding more strongly. Although at present we have no direct evidence for interaction between cations and olefins, such interactions in the case of aromatics via absorption, emission and solid state NMR studies have been established.

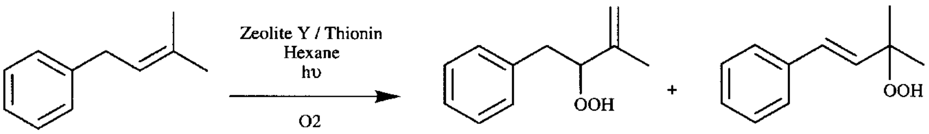

Cation	Cation radius	2°	3°
LiY / Thionin	0.76 Å	100	--
NaY / Thionin	1.02	85	15
RbY / Thionin	1.52	80	20
CsY / Thionin	1.67	66	34

Scheme 8.

Cation Interactions Restrict the Mobility of Reactants and Intermediates: Cation-Aromatic π-Interaction

Photo-Fries rearrangement of phenylacetate and photo-Claisen rearrangement of allylphenyl ether yield *ortho*-hydroxy and *para*-hydroxy isomers as products (Schemes 9 and 10) [45]. In solution, independent of the polarity of the medium, one obtains a mixture. On the other hand, zeolite once again comes handy to control the product distribution [46-50]. Remarkably, while in solution eight products are formed, within NaY zeolite a single product dominates the product mixture (Scheme 11).

Both photo-Fries and photo-Claisen rearrangements proceed *via* a similar mechanism (Scheme 12). Promotion to the excited singlet state results in fragmentation of the ester and the ether. Cage escape, recombination, and hydrogen migration result in both the *ortho-* and the *para*-isomers. However, the factors that control the outcome of the products vary with the nature of the medium. In solution, it is the electron densities at various aromatic carbons in the phenoxy radical which control the regioselectivity. Selectivity within zeolites, results from the restriction imposed on the mobility of the phenoxy and the acyl fragments by the supercage and the cations. Based on a comparison of the results observed in the case of phenylacetate and allylphenyl ether we believe that an interaction between the cation and the two reactive fragments is contributing to the observed selectivity. While the size and shape of the acyl and allyl radicals are expected to be similar, the strength of the interaction between the cations and these fragments will be different. The weaker binding of the allyl radical is translated to an increased yield of the para-isomer in the case of allylphenyl ether.

Recognition of the following features of the zeolite interior has helped us control site-selectivity during various photorearrangements: The cavity walls of zeolites, unlike those of many other organized media, are not ‘passive’. Cations present within zeolites help anchor the reactants, intermediates and products to the surfaces of a reaction cavity. In addition, the walls are very ‘hard’ so that the shapes and volumes of the cavities do not change during the time period of reactions.

The feature that distinguishes zeolite surfaces from silica

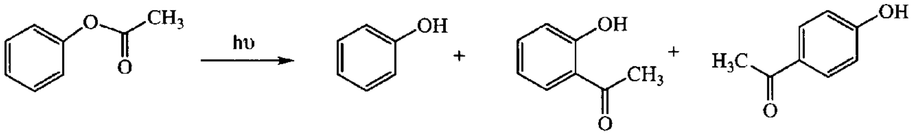

Hexane	20	53	27
Methanol	17	44	39
Na Y/hexane	5	91	4

Scheme 9.

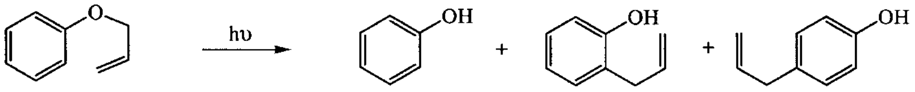

Hexane	48	21	31
Methanol	16	42	42
Na Y/hexane	3	79	18

Scheme 10.

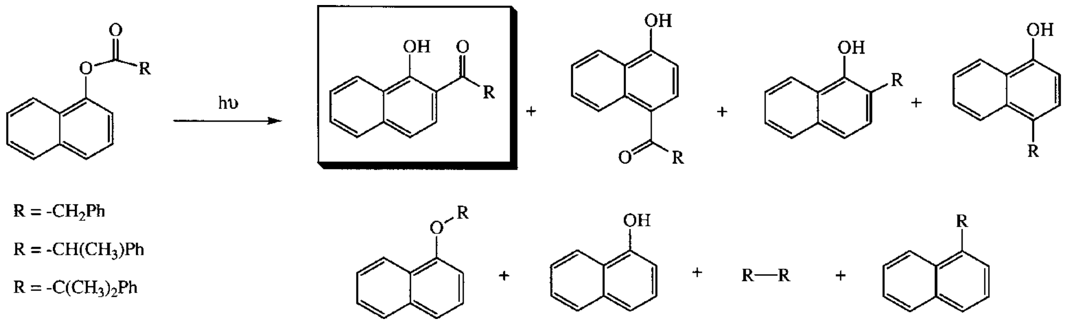

R = -CH$_2$Ph
R = -CH(CH$_3$)Ph
R = -C(CH$_3$)$_2$Ph

Scheme 11.

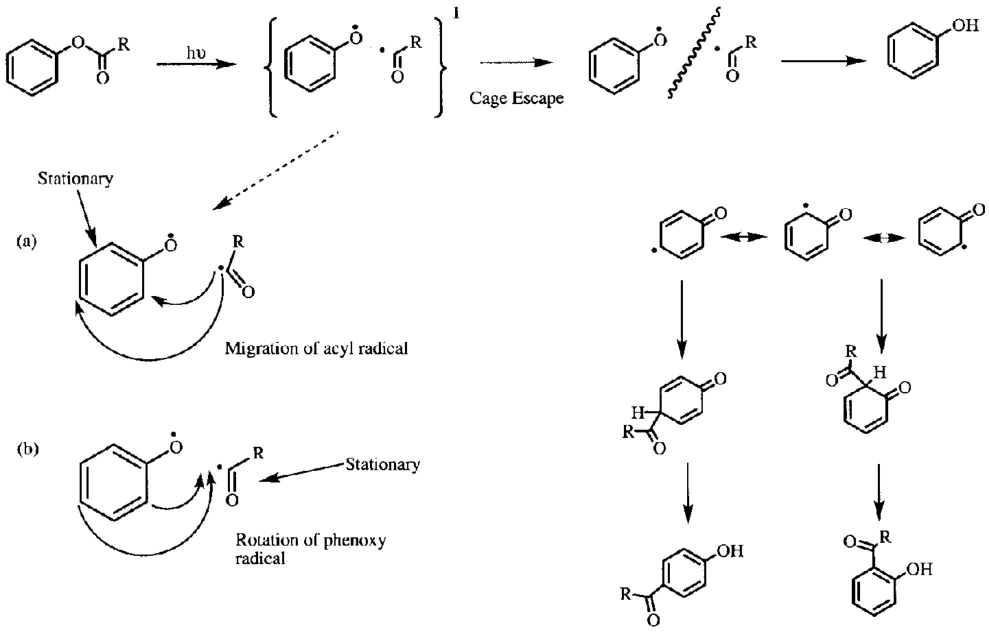

Scheme 12.

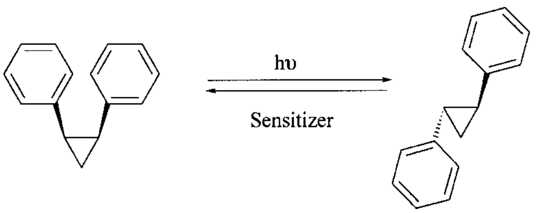

Scheme 13.

and alumina surfaces is the presence of cations. Although cations are embedded on the surface of a zeolite through interaction with surface oxygens, one face of these cations is free to interact with the guest molecules. We have exploited this feature to control the stereoisomers formed in a reaction. Diphenylcyclopropane upon triplet transfer sensitization yield a photostationary mixture consisting of nearly equal amounts of cis and trans isomers (Scheme 13) [51]. On the other hand, similar sensitizations (*para*-methoxy acetophenone) within a zeolite yield selectively the cis isomer. This remarkable one-way isomerization can not be achieved in solution even in presence of cations (acetonitrile-lithium perchlorate solution). Selective formation of the cis isomer depends on the nature of the cation (best results are achieved with lithium and sodium ions). Consideration of the structures of the cis and trans isomers provides a clue to the factor that might be involved in the formation of cis isomer within a zeolite. The cation is likely to complex more easily with the bowl shaped cis isomer than with the linear trans isomer (Scheme 13). This selective binding, we believe, is responsible for enrichment of the cis isomer at the photostationary state. This conclusion is consistent with the lower ratio of the cis isomer within wet NaY zeolite.

Enantioselective Photoreactions within Zeolites. Development and Establishment of the Concept and Generalizations

An ideal approach to achieving chiral induction in a constrained medium such as zeolite would be to make use of a chiral medium. To our knowledge no zeolite that can accommodate organic molecules, currently exists in a stable chiral form. Though zeolite beta and titanosilicate ETS-10 have unstable chiral polymorphs, no pure enantiomorphous forms have been isolated. Although many other zeolites can, theoretically, exist in chiral forms (e.g., ZSM-5 and ZSM-11) none has been isolated in such a state. In the absence of readily available chiral zeolites, we are left with the choice of creating an asymmetric environment within zeolites by the adsorption of chiral organic molecules.

In order to provide the asymmetric environment lacking in zeolites during the reaction a chiral source had to be employed. For this purpose, in the approach we refer to as the chiral inductor method (CIM), where optically pure chiral inductors such as ephedrine were used, the non-chiral surface of the zeolite becomes ‘locally chiral’ in the presence of a chiral inductor. This simple method affords easy isolation of the product as the chiral inductor and the reactant are not connected through either a covalent or an ionic bond. In all our studies alkali ion-exchanged zeolites X and Y were used as reaction media [52-68].

The chiral inductor that is used to modify the zeolite interior will determine the magnitude of the enantioselectivity of the photoproduct. The suitability of a chiral inductor for a particular study depends on its inertness under the given photochemical condition, its shape, size (in relation to that of the reactant molecule and the free volume of the zeolite cavity) and the nature of the interaction(s) that will develop between the

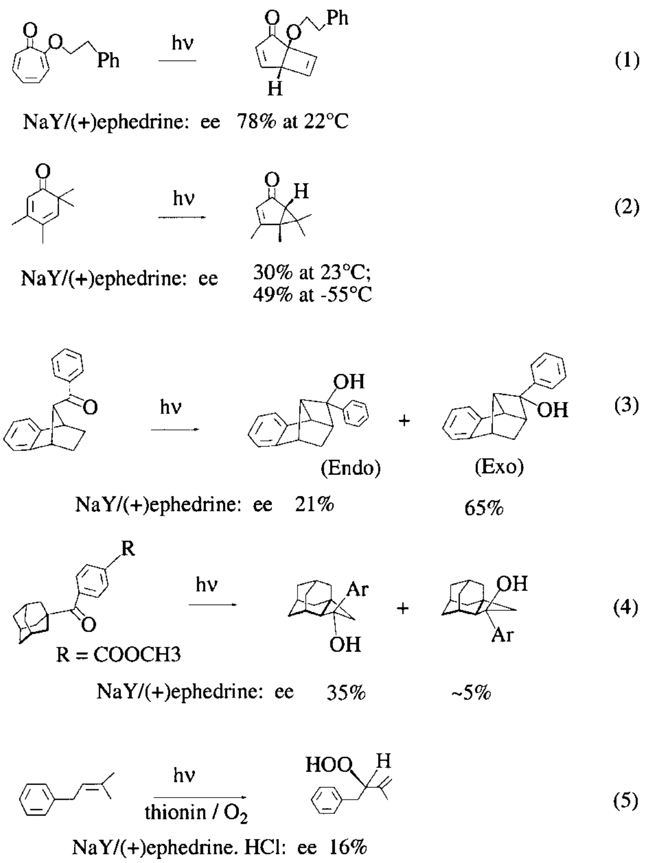

Scheme 14.

chiral agent and the reactant molecule/transition state/reactive intermediate. One should recognize that no single chiral agent might be ideal for two different reactions or at times structurally differing substrates undergoing the same reaction. These are inherent problems of chiral chemistry.

To examine the viability of CIM we have explored a number of photoreactions (electrocyclic reactions, Zimmerman (di-π) reaction, oxa-di-π-methane rearrangement, Yang cyclization, geometric isomerization of 1,2-diphenylcyclopropane derivatives, and Schenk-ene reaction) which yield racemic products even in presence of chiral inductors in solution (Scheme 14). We have obtained highly encouraging enantiomeric excesses (ee) on two photoreactions within NaY: photocyclization of tropolone ethylphenyl ether (eq. 1, Scheme 14). and Yang cyclization of phenyl benzonorbornyl ketone (eq. 3, Scheme 14). The ability of zeolites to drive a photoreaction that gives racemic products in solution to ee >60% provides hope of identifying conditions necessary to achieve high ee for a number of photoreactions with zeolite as a reaction medium. The following generalizations have resulted from the above studies: (a) Moderate but encouraging ee (15-70%) can be obtained in zeolites for systems that only result in racemic products in solution. (b) Not all chiral inductors work well within a zeolite. Best results are obtained with ephedrine, norephedrine and pseudoephedrine. (c) The extent of ee obtained is inversely related to the water content of the zeolite. (d) The ee depends on the nature of the alkali cation present in a zeolite. For example, the ee on photocyclization of tropolone ethylphenyl ether, within (+)-ephedrine adsorbed, various cation exchanged zeolites are as follows: LiY: 22%; NaY: 68%; KY: 11% and RbY: 2%.

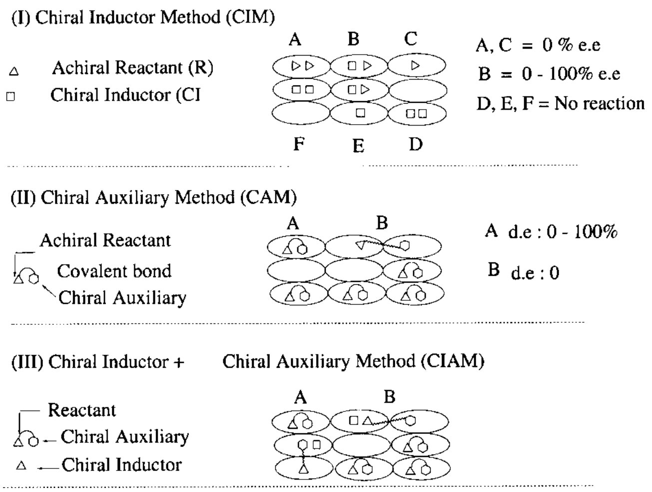

Scheme 15

The strategy of employing chirally modified zeolites as a reaction medium requiring the inclusion of two different molecules, a chiral inductor (CI) and a reactant (R), within the interior space of an achiral zeolite, by its very nature does not allow quantitative asymmetric induction. The expected six possible statistical distribution of the two different molecules CI and R when included within zeolites X and Y shown in Scheme 15-I are: cages containing two R molecules (type A), one R and one CI (type B), single R (type C), two CI (type D), a single CI (type E), and no CI and R molecules (type F). The products obtained from the photoreaction of R represent the sum of reactions that occur in cages of types A, B and C, of which, B alone leads to asymmetric induction.

Obtaining high asymmetric induction therefore requires the placement of every reactant molecule next to a chiral inductor molecule (type B situation); *i.e.*, enhancement of the ratio of type B cages to the sum of types A and C. This led us to explore the chiral auxiliary method (CAM) in which the chiral perturber is connected to the reactant via a covalent bond. In this approach, most cages are expected to contain both the reactant as well as the chiral inductor components within the same cage. We have tested the CAM with several reactions (electrocyclic reactions, oxa-di-π-methane rearrangement, Yang cyclization, and geometric isomerization of 1,2-diphenylcyclopropanes; for selected examples see Schemes 16 and 17) and have found that the diastereomeric excesses (de) obtained within zeolites are far superior to that in solution; de >75% have been obtained within MY zeolites for several systems which yield photoproducts in 1:1 diastereomeric ratio in solution. The observed generality suggests the phenomenon responsible for the enhanced asymmetric induction within zeolites to be

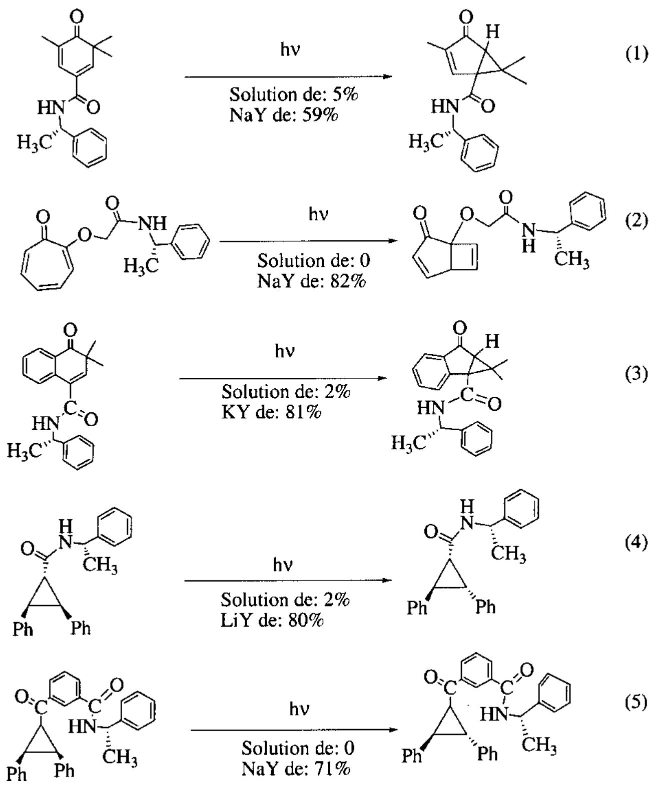

Scheme 16.

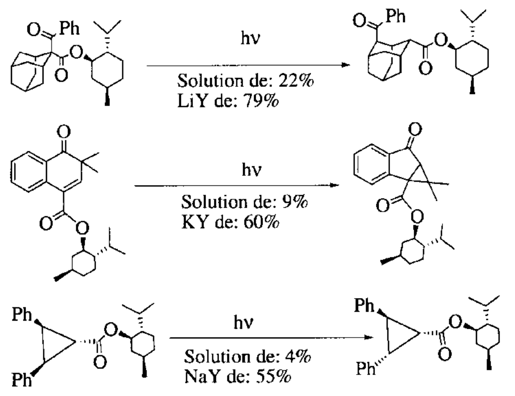

Scheme 17.

independent of the reaction. The GC traces of the photoproducts from tropolone 2-methyl-butyl ether (TMBE) and amide derived from L-valine methyl ester and 2β,3β-diphenylcyclopropane-1-α-carboxylic acid in various cation exchanged Y zeolites shown in Figures 21 and 22 illustrate that the cations present in a zeolite play a critical role in the asymmetric induction process and is further proved by the direct correlation of de on the water content of the zeolite. For example in the case of 1-phenylethyl amide of 2β,3β-diphenylcyclopropane-1α-carboxylic acid (Scheme 16, eq. 4) saturating the LiY with water dramatically reduced the de from 80% (dry) to 8% (wet). We believe that co-ordination of water to the cation reduces the influence of the cation on the reaction.

It is possible that the reactant and covalently linked chiral inductor still remain in different cages (type B in Scheme 15-II) by adopting an extended conformation that could result in <100% de. We have attempted to provide an asymmetric environment to such molecules by using a chirally modified Y

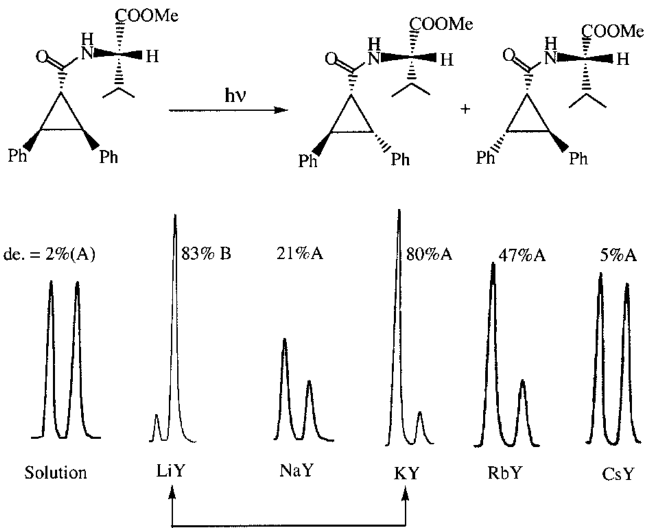

Figure 22. GC traces of the trans diastereomers of the amide derived from L-valine methyl ester and 2β,3β-diphenylcyclopropane-1α-carboxylic acid. Note the difference in the peaks being enhanced within LiY and KY.

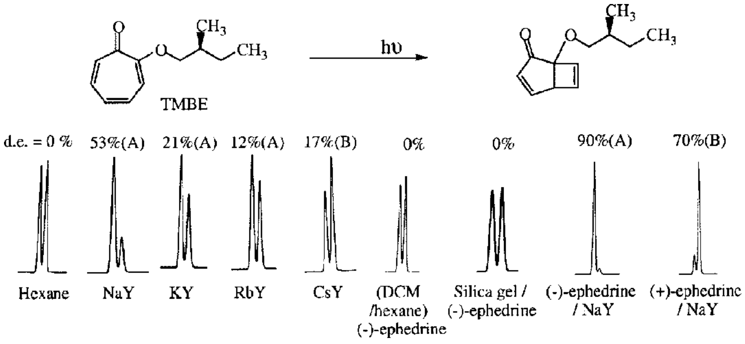

Figure 21. GC traces of the photoproducts from tropolone 2-methyl butyl ether, A refers to the first of the two peaks corresponding to product diastereomers.

zeolite as the reaction medium (Scheme 2-III; CIAM). Within (–)-ephedrine modified NaY the de with TMBE increased from 53% to 90% (Figure 1) while it decreased from 59% to 3% in the case of 1-phenylethylamide of 2,6,6-trimethylcyclohexa-2,4-diene-1-one-4-carboxylic acid (eq. 1 Scheme 16). Thus the combination of the chiral inductor and the chiral auxiliary has led to a limited success. However, the 90% de obtained with TMBE within (–)-ephedrine modified NaY is the highest thus far reported for any photochemical reaction in a non-crystalline medium. As shown in Figure 29 the 20% decrease in the maximum de obtained with (+)-ephedrine from that to its antipode (90% in (–)-ephedrine and 70% in (+)-ephedrine) suggests the reactions to occur in two types of cages, one that contains TMBE alone and the second that contains TMBE and a chiral inductor (type A and type B respectively in Scheme 15-III.

One of the drawbacks of the use of zeolite as a reaction medium is the difficulty in controlling the distribution of reactants and chiral inductors as illustrated in Scheme 15-I. This problem could be overcome by localizing the photoreaction to those cages in which the reactant is next to a chiral inductor (type B in Scheme 15-I). We have explored this concept with the photoreduction of ketones by amines as a probe reaction. The ketone we have examined is phenyl cyclohexyl ketone (Figure 23). This ketone upon excitation in solution gives an intramolecular γ-hydrogen abstraction Norrish type II product. However, when included within a chirally (ephedrine, pseudo-ephedrine or norephedrine) modified zeolite, it gave the intermolecular reduction product, α-cyclohexyl benzyl alcohol. The ratio of the intermolecular reduction to Norrish type II product was dependent on the nature (primary, secondary or tertiary) and amount of the chiral amine. These observations are indicative of the reduction occurring only in cages that contain a chiral inductor. Using norephedrine as the chiral inductor the ee obtained on the reduction product is 68% (Figure 23). As expected, the enhanced isomer is reversed with the antipode of the chiral inductor. It is important to note that under similar conditions in solution no ee was obtained in the reduction product. We have established the strategy presented above with phenyl cyclohexyl ketone to be general by investigating a number of aryl alkyl and diaryl ketones (Scheme 18). Despite the high ee obtained by this approach where entire reaction occurs within chirally modified cages, the %ee is not quantitative.

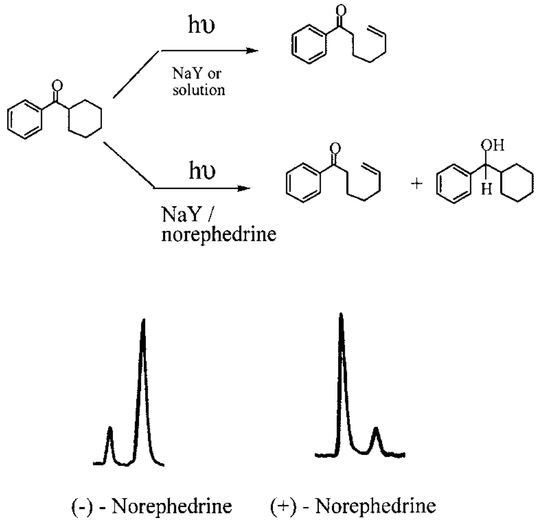

Figure 23. GC traces of the enantiomeric α-cyclohexyl benzyl alcohol. (+) and (-) Norephedrine enhances, as expected, opposite optical isomers.

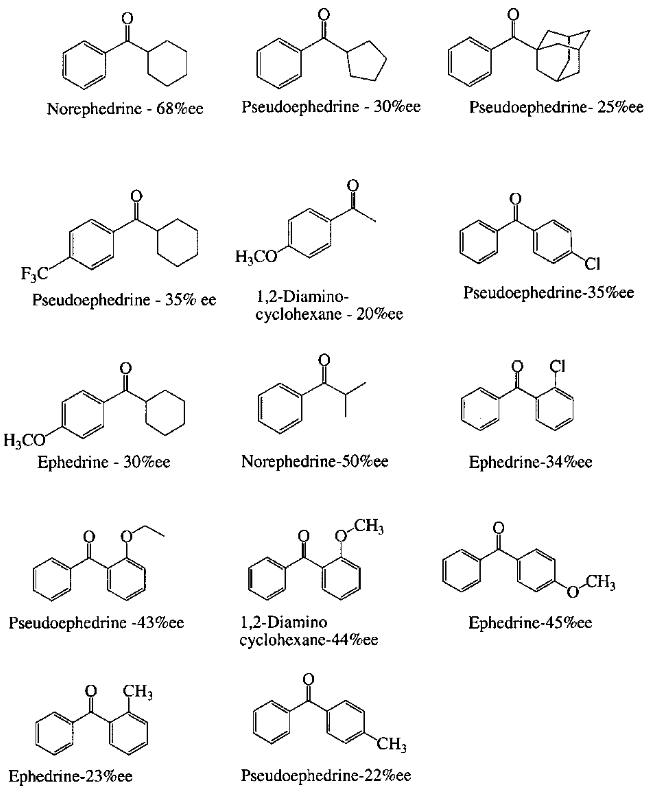

Scheme 18.

SUMMARY

During the past three decades a number of organized assemblies (micelles, vesicles, mono- and bilayers, liquid crystals, cyclodextrins, silica, clay and zeolite surfaces etc.) have been examined as media to control the excited state behavior of organic molecules. Each of them is unique in their ability to modify photoreactions. Zeolites are far more versatile in their ability to control reactions of a large variety of molecules. Zeolites are porous, highly interactive matrices. Zeolites serve as powerful matrices to monitor phosphorescence from molecules that do not phosphorescence under conventional conditions. Proton transfer and electron transfer are the two fundamental reactions that take place within a zeolite and most often zeolite matrix themselves participate in these reactions. Radical cations and carbocations generated via electron and proton transfer processes have long lifetime within a zeolite and thus lend themselves to be handled as ‘regular’ chemicals.

Cations being Lewis acids interact with π-electrons of included organic molecules and thus influence their location, adsorption mode and conformation. Such controls can be translated into product selectivity. ‘Naked’ cations within a zeolite provide an unprecedented opportunity to explore reactions catalyzed by cations. These cations are capable of polarizing π-electrons and thus may bring about reactions that are normally considered less likely in solution.

Ability to include two molecules within a supercage provides an opportunity to establish a communication between two molecules in an excited state. Such interactions have resulted in energy transfer, electron transfer and chiral induction. Of these chiral induction within zeolites is most unique and one is able to achieve high chiral induction in systems which yield racemic products in solution.

Acknowledgements – VR thanks the National Science Foundation (CHE-9904187 and CHE-0212042) for financial support. The work presented here is the result of enthuisiatic and co-ordinated efforts of K. Pitchumani, X. Li, G. Sundarababu, V. Jayathirtha Rao, R. J. Robbins, A. Joy, M. Warrier, P. Lakshminarasimhan, S. Uppili, J. Sivaguru, J. Shailaja, N. Arunkumar and L. S. Kaanumalle. Since their first meeting in 1980, friendship between Dr. S. C. Shim and VR grew steadily over a period of two decades. VR and the photochemical community dearly miss Dr. Shim to whose memory this article is dedicated.

REFERENCES

1. *Organic Chemistry in Anisotropic Media* (1987) Tetrahedron Symposium in Print #29, (edited by V. Ramamurthy, V., J. R. Scheffer and N. J. Turro), *Tetrahedron*, **43**, 1197-1745.
2. *Molecular Assembly and Reactivity of Organic Crystals and Related Structures*, Tetrahedron Symposium in Print #81, (2000) (edited by M. Garcia-Garibay, V. Ramamurthy and J. R. Scheffer), *Tetrahedron*, **56**, 6595-7049.
3. *Photochemistry in Organized and Constrained Media* (1991) (edited by V. Ramamurthy), VCH: New York.
4. Van-Bekkum, H., E. M. Flanigen and J. C. Jansen (1991) *Introduction to Zeolite Science and Practice*. Elsevier: Amsterdam.
5. Dyer, A. (1988) *An Introduction to Zeolite Molecular Sieves*. John Wiley and Sons: New York.
6. Breck, D. W. (1974) *Zeolite Molecular Sieves: Structure, Chemistry and Use*. John Wiley and Sons: New York.
7. *Advanced Zeolite Science and Applications* (1994) (editors, J. C. Jansen, M. Stocker, H. G. Karge and J. Weitkamp) Elsevier: Amsterdam.
8. *Inclusion Chemistry with Zeolites: Nanoscopic Materials by Design* (1995) (edited by N. Herron, and D. R. Corbin), Kluwer Academic Publishers: Dordrechet .
9. Weiss, R. G., V. Ramamurthy and G. S. Hammond (1993) Photochemistry in Organized and Confining Media: A Model. *Acc. Chem. Res.*, **26**, 530-536.
10. Ramamurthy, V., R. G. Weiss and G. S. Hammond (1993) A Model for the Influence of Organized Media on Photochemical Reactions. *Ad. Photochem*. **18**, 67-234
11. Cohen, M. D. (1975) The Photochemistry of Organic Solids. *Angew. Chem. Int. Ed. Engl.* **14**, 386-393.
12. Calculations of polyhedral volumes were performed using a modification of the POLYVOL Program [D Swanson, RC Peterson. The Canadian Mineralogist. **18**(2): 153, 1980. DK Swanson, RC Peterson. “POLYVOL Program Documentation”, Virginia Polytechnic Institute, Blacksburg, VA] assuming the radius of the TO_2 unit to be 2.08 Å (equivalent to that of quartz).
13. Turro. N. J. (1978) *Modern Molecular Photochemistry*, University Science Books: Mill Valley.
14. For a brief history: P. Pringsheim and M. Vogel (1943) *Luminescence of Liquids and Solids*, Interscience Publishers: New York.
15. Murov, S. L., I. Carmichael and G. L. Hug (1993) *Handbook of Photochemistry*, Second edition, Marcel and Dekker: New York, 294-297.
16. Hurtubise, R. J. (1990) *Phosphorimetry*. VCH: New York.
17. Vo-Dinh. T. (1984) *Room Temperature Phosphorimetry for Chemical Analysis*. New York: Wiley-Interscience.
18. Ramamurthy, V., J. V. Caspar, E. W. Kuo, D. R. Corbin and D. F. Eaton (1992) Heavy Atom Induced Phosphorescence of Aromatics and Olefins Included within Zeolites. *J. Am. Chem. Soc*. **114**, 3882-3892.
19. Ramamurthy, V., J. V Caspar, D. R. Corbin and D. F. Eaton (1989) Modification of photochemical reactivity by zeolites: Location of guests within faujasites by heavy atom induced phosphorescence. *J Photochem Photobiol A: Chemistry*, **50**, 157-161.
20. Caspar, J. V., V. Ramamurthy and D. R Corbin (1990) The location of guests within X-type faujasite zeolites via external heavy atom induced phosphorescence. *Coord. Chem. Rev.* **97**, 225-236.
21. Ramamurthy, V., J. V. Caspar and D. R. Corbin (1990) Modification of photochemical reactivity by zeolites: Heavy cation induced phosphorescence and entrapment of rotational conformers of *trans*-stilbene. *Tetrahedron Letters*, **31**, 1097-1100.
22. Ramamurthy, V., J. V. Caspar, D. R. Corbin, B. D. Schlyer and A. H. Maki (1990) Triplet state photophysics of naphthalene and α,ω-diphenylpolyenes included in heavy cation exchanged zeolites. *J. Phys. Chem*. **94**, 3391-3393.
23. Lower, S. K. and M. El Sayed (1966) The triplet state and Molecular Electronic Processes in Organic Molecules. *Chem. Rev.* **66**, 199-241.
24. Uppili, S., V. Marti, A. Nikolaus, W. Adam, P. S. Engel, N. J. Turro and V. Ramamurthy (2000) Heavy-Cation-Induced Phosphorescence of Alkanones and Azoalkanes In Zeolites

As Hosts: Induced S_1 ($n\pi^*$) to T_1 ($n\pi^*$) Intersystem Crossing and S_0 to T_1 ($n\pi^*$) Absorption. *J. Am. Chem. Soc.* **122**, 11025-11026.

25. Werst, D. W. and A. D. Trifunac (1998) Observation of Radical Ions by Swiftness or Stealth. *Acc. Chem. Res.* **31**, 651-657.
26. Caspar, J. V., V. Ramamurthy and D. R. Corbin (1991) Preparation and spectroscopic characterization of polarons and bipolarons of thiophene oligomers within the channels of pentasil zeolites: The evolution of organic radical ions into conducting polymers. *J. Am. Chem. Soc.* **113**, 600-610.
27. Ramamurthy, V., J. V. Caspar and D. R Corbin (1991) Generation, entrapment and spectroscopic characterization of radical cations of α,ω-diphenylpolyenes within the channels of pentasil zeolites. *J. Am. Chem. Soc.* **113**, 594-600.
28. Ramamurthy, V. (1992) Photochemistry and Photophysics within Zeolites. *Chimia*, **46**, 359-376.
29. Ramamurthy, V., D. F. Eaton and J. V Caspar (1992) Photochemistry and Photophysics of Organic Molecules Included within Zeolites. *Acc Chem Res.* **25**, 299-307.
30. Pitchumani K. and V. Ramamurthy (1996) Exceptionally Stable Carbocation from Indene Generated and Trapped within Ca Y Zeolite. *J. Chem. Soc. Chem. Commun.* 2763-2764.
31. Jayathirtha Rao, V., N. Prevost, V. Ramamurthy, M. Kojima and L. J. Johnston (1997) Generation of Stable and Persistent Carbocations From 4-Vinylanisole Within Zeolites. *J. Chem. Soc. Chem. Commun.* 2209-2210.
32. Pitchumani, K., P. H. Lakshminarasimhan, N. Prevost, D. R. Corbin and V. Ramamurthy (1997) *J. Chem. Soc. Chem. Commun.* 181-182.
33. Pitchumani, K., A. Joy, N. Prevost and V. Ramamurthy (1997) Zeolite as a Reagent and as a Catalyst: Reduction and Isomerization of Stilbenes by CaY. *J. Chem. Soc. Chem. Commun.* 127-128.
34. Pitchumani, K., P. H. Lakshminarasimhan, G. Turner, M. G. Bakker and V. Ramamurthy (1997) Cation Radical and Carbocation Mediated Reactions within CaY Zeolite: 1-Phenyl 3,4-dihydronaphthalene. *Tetrahedron Letters,* **38**, 371-374.
35. Pitchumani, K., D. R. Corbin and V. Ramamurthy (1996) Electron Transfer Reactions within Zeolites: Radical Cations from Benzonorbornadiene and Dibenzobarrelene. *J. Am. Chem. Soc.* **118**, 8152-8153.
36. Ramamurthy, V., P. H. Lakshminarasimhan, C. P. Grey and L. J. Johnston (1998) Energy Transfer, Proton Transfer and Electron Transfer Reactions Within Zeolites. *J. Chem. Soc. Chem. Commun.* 2411-2424.
37. Lakshminarasimhan, P. H., K. J. Thomas, L. Brancaleon, P. D. Wood, L. J. Johnston and V. Ramamurthy (1999) Characterization of persistnt intermediates generated upon inclusion of 1,1-diarylethylenes within CaY: Spectroscopy and Product Studies. *J. Phys. Chem. B.* **103**, 9247-9254.
38. Jayathirtha Rao, V., S. Uppili, D. R. Corbin, S. Schwarz, S. R. Lustig and V. Ramamurthy (1998) Facial Selective Photoreduction of Steroids: Role of Zeolites. *J. Am. Chem. Soc.* **120**, 2480-2481.
39. Uppili, S., S. Takagi, R. B. Sunoj, P. H. Lakshminarasimhan, J. Chandrasekhar and V. Ramamurthy (2001) Controlling the Reactive State Through Cation Binding: Photochemistry of Enones within Zeolites. *Tetrahedron Letters,* **42**, 2079-2083.
40. Sunoj, R. B., P. H. Lakshminarasimhan, V. Ramamurthy and J. Chandrasekhar (2001) Configuration Interaction and Density Functional Study of the Influence of Lithium Cation Complexation on Vertical and Adiabatic Excitation Energies of Enones. *J Comput. Chem.* **22**, 1598-1604.
41. Uppili, S., K. J. Thomas, E. Crompton and V. Ramamurthy (2000) Probing zeolites with organic molecules: Supercages of X and Y zeolites are superpolar. *Langmuir,* **16**, 265-274.
42. Li, X. and V. Ramamurthy (1996) Selective Oxidation of Olefins within Organic Cation Exchanged Zeolites. *J. Am. Chem. Soc.* **118**, 10666-10667.
43. Robbins, R. and V. Ramamurthy (1997) Generation and Reactivity of Singlet Oxygen Within Zeolites: Remarkable Control of hydroperoxidation of alkenes. *J. Chem. Soc. Chem. Commun.* 1071-1072.
44. Shailaja, J., J. Sivaguru, R. J. Robbins, V. Ramamurthy, R. B. Sunoj and J. Chandrasekhar (2000) Singlet Oxygen Mediated Oxidation of Olefins Within Zeolites: Selectivity and Complexities. *Tetrahedron,* **56**, 6927-6943.
45. Pitchumani, K., M. Warrier and V. Ramamurthy (1996) Remarkable Product Selectivity During Photo-Fries and Photo-Claisen Rearrnagements within Zeolites. *J. Am. Chem. Soc.* **118**, 9428-9429.
46. Pitchumani, K., M. Warrier, C. Cui, R. G. Weiss and V. Ramamurthy (1996) Photo-Fries Reaction of Naphthyl Esters within Zeolites. *Tetrahedron Letters,* **37**, 6251-6254.
47. Pitchumani, K., M. Warrier and V. Ramamurthy (1999) Utility of zeolitic medium in photo-Fries and photo-Claisen rearrangements. *Res. Chem. Intermediates,* **25**, 623-631.
48. Gu, W., M. Warrier, V. Ramamurthy and R. G. Weiss (1999) Photo-Fries reactions of 1-naphthyl esters in cation exchanged zeolite Y and polyethylene media. *J. Am. Chem. Soc.* **121**, 9467-9468.
49. Joy, A., M. Warrier and V. Ramamurthy (2000) Enforcing molecules to behave. *Spectrum,* **12**(3), 1-8.
50. Gu, W., M. Warrier, B. Schoon,V. Ramamurthy and R. G. Weiss (2000) Understanding the Influence of Active (Zeolite) and Passive (Polyethylene) Reaction Cages on Photo-Claisen Rearrangements of Aryl Benzyl Ethers. *Langmuir,* **16**, 6977-6981.
51. Lakshminarasimhan, P. H., R. B. Sunoj, J. Chandrasekhar and V Ramamurthy (2000) Cation-π Interaction Controlled One-Way Geometric Photoisomerization of Diphenyl-cyclopropane. *J. Am. Chem. Soc.* **122**, 4815-4816.
52. Joy, A., R. J. Robbins, K. Pitchumani and V. Ramamurthy (1997) Asymmetrically Modified Zeolite As a Medium For Enantioselective Photoreactions: Reactions From Spin Forbidden Excited States. *Tetrahedron Letters,* 8825-8828.
53. Sundarababu, G., M. Leibovitch, D. R. Corbin, J. R. Scheffer and V. Ramamurthy (1996) Zeolite as a host for chiral induction. *J. Chem. Soc Chem. Comm.* 2159-2160.
54. Leibovitch, M., G. Olovsson, G. Sundarababu, V. Ramamurthy, J. R. Scheffer and J. Trotter (1996) Asymmetric Induction in

Photochemical Reactions Conducted in Zeolites and in the Crystalline State. *J. Am. Chem. Soc*. **118**, 1219-1220.

55. Joy, A., J. R. Scheffer, D. R. Corbin and V. Ramamurthy (1998) Enantio Selective Photocyclization within Zeolites: Tropolone methyl ether in Chirally Modified Zeolites. *J. Chem. Soc. Chem. Commun.* 1379-1380.
56. Joy, A., D. R. Corbin and V. Ramamurthy (1999) Studies on Chiral Induction within Zeolites: Photoelectrocyclization of Tropolone alkylethers. In Proceedings of 12th International Zeolite Conference. (edited by M. M. J. Traecy, B. K. Marcus, B. E. Bisher and J. B Higgins). 2095-2102. Materials Research Society: Warrendale, PA, 2095.
57. Joy, A. and V. Ramamurthy (2000) Chiral photochemistry within zeolites. *Chemistry Eur J*. **6**, 1287-1293.
58. Joy, A., S. Uppili, M. R. Netherton, J. R. Scheffer and V. Ramamurthy (2000) Photochemistry of Tropolone ethers and 2,2-dimethyl-1-(2H)-naphthalenones Within a Zeolite: Chiral Amplification Via Confinement. *J. Am. Chem. Soc*. **122**, 728-729.
59. Joy, A., J. R. Scheffer and V. Ramamurthy (2000) Chirally Modified Zeolite as a Reaction Medium: Photochemistry of an Achiral Tropolone ether. *Org. Letters*, **2**, 119-122.
60. Shailaja, J., K. J. Ponchot and V. Ramamurthy (2000) Enantioselective Photoreduction of arylalkyl ketones via restricting the reaction to chirally modified zeolites. *Org. Letters*, **2**, 937-940.
61. Cheung, E., K. C. W. Chong, S. Jayaraman, V. Ramamurthy, J. R. Scheffer and J. Trotter (2000) Enantio- and diastereo-differentiating *cis,trans*-photoisomerization of 2β,3β-di-phenylcyclopropane-1α-carboxylic acid derivatives in organized media. *Org Letters* **2**, 2801-2804.
62. Jayaraman, S., S. Uppili, A. Natarajan, A. Joy, K. C. W. Chong, M. R. Netherton, A. Zenova, J. R. Scheffer and V. Ramamurthy (2000) Influence Of Chiral Auxiliaries Is Enhanced Within Zeolites. *Tetrahedron Letters*, **41**, 8231-6235.
63. Shailaja, J., J. Sivaguru, S. Uppili, A. Joy and V. Ramamurthy (2001) Use of a Confined Space (Zeolite) in Enatio and Distereoselective Photoreactions. *Microporous and Mesoporous Materials*, **48**, 319-328.
64. Sivaguru, J., J. Shailaja, S. Uppili, K. Ponchot, A. Joy, N. Arunkumar and V. Ramamurthy (2002) Achieving Enantio and Diastereoselectivities in Photoreactions Through the Use of a Confined Space. In Organic Solid State Reactions (edited by F Toda) 159-188. Kluwer Academic Press: Amsterdam.
65. Chong, K. C. W., S. Jayaraman, T. Shichi, Y. Yoshimi, V. Ramamurthy and J. R. Scheffer (2002) Use of Chirally Modified Zeolites and Crystals in Photochemical Asymmetric Synthesis. *J. Am. Chem. Soc*. **124**, 2858-2859.
66. Uppili, S. and V. Ramamurthy (2002) Enhanced Enantio- and Diastereoselectivities via Confinement: Photorearrangement of 2,4-Cyclohexadienones Included in Zeolites. *Org Letters*, **4**, 87-90.
67. Sivaguru, J. J. R. Scheffer, and V. Ramamurthy (2002) Confined Space and Cations Enhance the Power of a Chiral Auxiliary: Photochemistry of 1,2-Diphenylcyclopropane Derivatives. *J. Chem. Soc. Chem. Commun*. 830-831.
68. Arunkumar, N., K. Wang, V. Ramamurthy and J. R. Scheffer (2002) Control of Enantioselectivity in the Photochemical Conversion of α-Oxoamides into β-Lactam Derivatives. *Org Letters*, **4**, 1443-1446.